Additional Information

Developmental role of the tomato Mediator complex subunit MED18 in pollen ontogeny

Fernando Pérez-Martín[1], Fernando J. Yuste-Lisbona[1], Benito Pineda[2], Begoña García-Sogo[2], Iván del Olmo[3], Juan de Dios Alché[4], Isabel Egea[5], Francisco B. Flores[5], Manuel Piñeiro[3], José A. Jarillo[3], Trinidad Angosto[1], Juan Capel[1], Vicente Moreno[2] and Rafael Lozano[1, *]

[1] Centro de Investigación en Biotecnología Agroalimentaria (BITAL). Universidad de Almería, 04120 Almería, Spain.

[2] Instituto de Biología Molecular y Celular de Plantas, Universidad Politécnica de Valencia-CSIC, 46022 Valencia, Spain.

[3] Centro de Biotecnología y Genómica de Plantas, Universidad Politécnica de Madrid (UPM) - Instituto Nacional de Investigación y Tecnología Agraria y Alimentaria (INIA), Campus Montegancedo UPM, 28223 Pozuelo de Alarcón (Madrid), Spain

[4] Departamento de Bioquímica, Biología Celular y Molecular de Plantas, EEZ-CSIC, 18008 Granada, Spain.

[5] Departamento de Biología del Estrés y Patología Vegetal, CEBAS-CSIC, 30100 Espinardo-Murcia, Spain

* Corresponding author: rlozano@ual.es

Prof. Rafael Lozano

Dept. Biología y Geología

Edificio Científico-Técnico II-B

Universidad de Almería

04120 Almería, Spain

Tel. +34 950 01 5111

Fax +34 950 01 5476

Running head: Function of *SlMED18* in pollen development

Key words: Tomato, pollen development, tapetum degradation, Mediator complex, T-DNA insertional mutagenesis.

Word count: 7258

Summary

Pollen development is a crucial step in higher plants which not only makes possible plant fertilization and seed formation, but also determine fruit quality and yield in crop species. Here, we reported a tomato T-DNA mutant, *pollen deficient1* (*pod1*), characterized by an abnormal anther development and the lack of viable pollen formation, which led to the production of parthenocarpic fruits. Genomic analyses and the characterization of silencing lines proved that *pod1* mutant phenotype relies on the tomato *SlMED18* gene encoding the subunit 18 of Mediator multi-protein complex involved in RNA polymerase II transcription machinery. The loss of *SlMED18* function delayed tapetum degeneration, which resulted in deficient microspore development and scarce production of viable pollen. A detailed histological characterization of anther development proved that changes during microgametogenesis and a significant delay in tapetum degeneration are associated with a high proportion of degenerated cells and hence, should be responsible for the low production of functional pollen grains. Expression of pollen marker genes indicated that *SlMED18* is essential for the proper transcription of a subset of genes specifically required to pollen formation and fruit development, revealing a key role of *SlMED18* in male gametogenesis of tomato. Additionally, *SlMED18* is able to rescue developmental abnormalities of the Arabidopsis *med18* mutant indicating that most biological functions have been conserved in both species.

Introduction

Pollination and fertilization of angiosperms are coordinated processes which allow the conversion of gynoecium into a seeded fruit and therefore, are essential events to ensure species survival and fruit yield (Gillaspy *et al*., 1993; Ozga and Reinecke, 2003; Carbonell-Bejerano *et al*., 2010, Lora *et al*., 2011). Thus, pollen development and maturation comprises multiple cellular changes mediated by a precisely orchestrated gene expression regulation (Honys and Twell, 2004; Pina *et al*., 2005; Wilson and Zhang, 2009; Feng *et al*., 2012; Rutley and Twell, 2015). Male gametogenesis takes place in anthers, where diploid archesporial cells divide into two cell layers with different fates: i) the primary parietal layer, which gives rise to four different cell layers by successive divisions, to form concentric layers of pollen sac wall, i.e. epidermis, endothecium, middle layer and tapetum; and ii) the primary sporogenous layer, which undergoes a small number of divisions to produce pollen mother cells (PMCs). These undifferentiated cells undergo meiosis leading to the formation of tetrads of haploid cells, which are released as free microspores. Finally, uninucleate microspores mature after an asymmetric mitotic division to produce pollen grains, which in turn enclose the vegetative and the generative cells (Scott *et al*., 2004).

Significant progress in understanding the genetic and molecular basis of pollen development has been made from the study of mutants in the model species *Arabidopsis thaliana*. Thus, mutations affecting several stages of pollen ontogeny have been identified, which have led to the isolation and functional analysis of several genes involved in pollen development. For instance, *sporocyteless/nozzle* (*spl/nzz*) mutant fails to form sporogenous tissue during early anther development. *SPL/NZZ* encodes a MADS-box transcription factor that plays a central role in regulating anther cell differentiation (Schiefthaler *et al*., 1999; Yang *et al*., 1999; Liu *et al*., 2009). In the case of *switch1* (*swi1*) mutant, male gametogenesis is affected during meiosis of PMCs. *SWI1* encodes a novel protein involved in sister chromatid cohesion and meiotic chromosome organization during both male and female meiosis (Mercier *et al*., 2003). Likewise, during microgametogenesis, the programmed cell death of the tapetum tissue is essential for proper pollen development, as it supplies nutrients to the microspores, as well as for regulating microspores release (Pacini, 2010). Consequently, mutations that disrupt tapetum ontology and promote aborted microgametogenesis causing male sterility have been reported, mainly *extra sporogenous cells/excess microsporocytes1* (*ems1/exs*), *tapetal determinant1* (*tpd1*), *aborted microspores* (*ams*) and *male sterility1*

3

(*ms1*) mutations. *EMS1/EXS* and *TPD1* genes encode a putative LRR receptor kinase and a small putatively-secreted protein, respectively, both required for specifying tapetal identity (Canales *et al*., 2002; Zhao *et al*., 2002; Yang *et al*., 2003). On the other hand, *AMS* gene encodes a transcription factor belonging to the MYC subfamily of bHLH genes, which is required for tapetal cell development in Arabidopsis (Sorensen *et al*., 2003). Similarly, *ms1* mutant pollen degenerates after microspore release due to an abnormal vacuolization of the tapetum (Wilson *et al*., 2001). Therefore, *MS1,* which encodes a PHD-finger class of transcription factors, is a key gene required for correct tapetum degradation (Yang *et al*., 2007).

In tomato, pollen development and the predetermined tapetum degeneration processes are quite similar to that of Arabidopsis (Polowick and Sawhney, 1993a,b; Brukhin *et al*., 2003; Wilson and Zhang, 2009). Tomato male sterility has been the subject of genetic research since it was first described by Crane (1915), whereupon more than 50 tomato male sterile mutants have been reported (Gorman and McCormick, 1997); however, in contrast to Arabidopsis, a small number of pollen development related genes have been identified so far. Among them, the tomato homologue to the Arabidopsis *ECERIFERUM6* (*CER6*) gene, which encodes a β-ketoacyl-coenzyme A synthase, is involved in the regulation of timely tapetum degradation (Smirnova *et al*., 2013). Recently, it has been demonstrated that *Male sterile 10^{35}* (*Ms10^{35}*) gene encodes a basic helix-loop-helix transcription factor, which participates in regulating both meiosis and programmed cell death of the tapetum during microsporogenesis (Jeong *et al*., 2014). Likewise, the glycine-rich protein LeGRP92 is essential for normal pollen function and survival as it facilitates the outer cell wall (or exine) formation (McNeil and Smith, 2010). Similarly, the *LATE ANTHER TOMATO 52* (*LAT52*) gene, encoding a heat-stable glycosylated protein, plays a crucial role in pollen hydration and germination (Muschietti *et al*., 1994).

Given the relevance of male sterility and fruit set for tomato breeding, a collection of tomato T-DNA insertion lines generated by an enhancer trap was screened (Pérez-Martín *et al*., 2017) aiming to identify new regulators involved in male fertility. This work describes the characterization of a tomato T-DNA mutant, *pollen deficient1* (*pod1*), which displayed a significant reduction of pollen viability that yielded parthenocarpic fruits. Functional analyses demonstrated that the loss of *MEDIATOR COMPLEX SUBUNIT 18* (*POD1/SlMED18*) function is responsible for the observed *pod1* phenotypic alterations. MED18 is a subunit of the MEDIATOR COMPLEX that

4

binds RNA Polymerase II, an evolutionarily conserved transcriptional regulatory complex of class II genes in all eukaryotes (Kornberg *et al*., 2005; Bourbon, 2008). Depending on the species, MEDIATOR is a large multimeric protein comprising 25-34 subunits (Allen and Taatjes, 2015; Samanta and Thakur, 2015), which are organised in four modules: head, middle, tail and CDK/Cycline (Chadick and Asturias, 2005; Conaway *et al*., 2005). Each subunit seems to be a specific regulator for defined gene sets related to different functions involved in gene transcription mediated by RNA Polymerase II, including transcription, initiation, and elongation, as well as RNA processing, chromatin spatial conformation and enhancer-promoter interaction (Buendía-Monreal and Gillmor, 2016).

In Arabidopsis, *MED18* is involved in the transcriptional response to different physiological and cellular processes, like plant immunity (Lai *et al*., 2014), flowering time and floral organ identity (Zheng *et al*., 2013). Recently, Wang *et al*. (2018) have reported the function of tomato *MED18* in regulating the development of leaf and stem. However, little is known about the role of *MED18* in reproductive development. This study reports a key function of *MED18* in pollen ontogeny, which is required to ensure a proper differentiation and maturation of pollen grains and tapetum degradation in tomato.

RESULTS

Phenotypic and genetic analysis of the *pollen deficient 1* (*pod1*) mutant

The *pod1* mutant was isolated from the screening of a collection of enhancer trap lines in the tomato cv. Moneymaker. Mutant plants were mainly affected in flower development. At anthesis stage, flowers showed a significant decrease in the length of petals, stamens and pistils of *pod1* flowers (Figure 1b; Table S1). About 10% of *pod1* flowers displayed different degrees of homeotic changes, from near to wild-type (WT) to aberrant phenotypes, which affected floral organs of the second and mainly the third whorls, indicating incomplete penetrance and variable expressivity of *pod1* mutation. Indeed, scanning electron microscopy (SEM) analysis showed the development of trichomes on the adaxial surface of some petals, a feature never observed in WT petals, as well as increased size of epidermal cells (Figure S1a,b). Moreover, a range of homeotic phenotypic alterations was observed from normal stamens to full conversion of stamens into carpels in the third whorl (Figure S1c,d), where the latter ones showed dramatic changes in size and shape of their epidermal cells compared to WT ones

(Figure S1e,f). Thus, both types of *pod1* stamens, with full and without any homeotic conversion, were subjected to qRT-PCR analysis. Three tomato B-class identity genes were assessed, i.e, *STAMENLESS* (*SL*), *TOMATO MADS6* (*TM6*) and *TOMATO PISTILLATA* (*TPI*), and significant down-regulation of all of them was observed in *pod1* stamens showing homeotic changes (Figure S1g). However, the expression of *TOMATO AGAMOUS 1* (*TAG1*), a C-class identity gene, was not altered in stamens of *pod1* plants (Figure S1g).

Stamens developed by *pod1* flowers showed a significant reduction in the amount (~5-fold) and viability (~20-fold) of pollen grains as compared to WT ones (Figure 1c,d; Table S1). An *in vivo* pollen germination assay was also performed through reciprocal crosses, which showed that WT pollen grains germinated and developed normal pollen tubes on stigmas of *pod1* flowers (Figure 1e); however, *pod1* pollen grains were unable to form pollen tubes on WT stigmas (Figure 1f). WT pollen was used in cross-pollination assays which yielded normal-seeded fruits, indicating that *pod1* mutation did not affect ovule functionality. However, selfing of *pod1* plants gave rise to small and parthenocarpic fruits, which showed reduced axial and equatorial diameters as well as decreased fresh weight compared to WT fruits (Figure 1g; Table S1).

In addition, vegetative developmental traits were also altered in *pod1* mutant plants, mainly a significant reduction in fresh weight and leaf length compared to WT plants, as well as a decreased development of secondary and tertiary leaflets, and reduced length of petioles (Figure 1a; Table S1). Such alterations coincide with those reported by Wang et al. (2018).

A genetic analysis of *pod1* mutant phenotype was performed on 411 segregating plants from two different progenies, 96 T2 and 315 T3 plants. The mutant phenotype was observed in 25 out of 96 T2 plants (26.04%) and 81 out of 315 T3 plants (25.71%). The Chi-square statistic test confirmed that segregation ratios were consistent with a monogenic autosomal recessive mode of inheritance for the *pod1* mutant phenotype (χ^2 = 0.14, *P* = 0.71).

Cloning and molecular characterization of the *pod1* mutant locus

Southern blot hybridization indicated that a single copy of T-DNA was inserted in the *pod1* genome (Figure 1h). Afterwards, with the aim to isolate the gene harbouring *pod1* mutation, anchor-PCR assays were performed to clone the genomic regions flanking the

T-DNA insertion. Results revealed that T-DNA was located on chromosome 06 (at position 1,860,352 bp; ITAG2.50), in the promoter region of two adjacent genes transcribed in opposite direction, the *MEDIATOR COMPLEX SUBUNIT 18* (*SlMED18*) gene (*Solyc06g008010*) and a tomato member of the Zinc Finger HIT-type (ZNHIT) transcription factor family (*Solyc06g008020*). Specifically, the T-DNA was inserted 482 bp upstream of the 5′-untranslated region of the *SlMED18* gene and 203 bp upstream of the translation start codon of the *ZNHIT* gene. The T-DNA insertion produced a deletion of 160 bp which affected the promoter region of both *SlMED18* and *ZNHIT* genes (Figure 1i).

To establish a possible correlation between the T-DNA insertion site in the genome with the *pod1* phenotype, a co-segregation analysis was performed by PCR in 411 plants from T2 and T3 progenies, which revealed that a total of 106 mutant plants (25.80%), 25 from T2 and 81 from T3, were homozygous for the T-DNA insertion, whereas 201 of the 305 WT plants (48.90%) were hemizygous and the remaining 104 WT plants (25.30%) were azygous for the T-DNA insertion (Figure 1j). Therefore, results of co-segregation analysis supported that the *pod1* phenotype was linked to the T-DNA insertion.

Given the genomic position of the T-DNA insertion, qRT-PCR experiments were carried out in *pod1* and WT plants to determine whether the *pod1* mutation affected the expression of *SlMED18* and *ZNHIT* genes. Results showed that both *SlMED18* and *ZNHIT* genes were down-regulated in all *pod1* tissues here analysed, i.e. root, stem, leaf, apex and flower at anthesis (Figure 1k,l).

Phenotype of *SlMED18* silencing plants resembles *pod1* mutant

To conclude which of the two candidate genes affected by the T-DNA insertion was responsible for *pod1* mutant phenotype, single and double RNAi silencing lines for *SlMED18* and *ZNHIT* genes were generated, being the latter ones used to evaluate the hypothesis that simultaneous down-regulation of both genes could be responsible for *pod1* mutant phenotype. qRT-PCR analysis proved that gene silencing specifically affected the gene (or genes) targeted in each type of RNAi line (Figure 2d; Figure S2a-c). Phenotypic characterization of representative RNAi lines revealed that developmental alterations of both RNAi *SlMED18* and double RNAi transgenic plants were similar to those of *pod1* plants (Table S1). Indeed, these transgenic flowers were also smaller displaying shortened stamens and narrow petals as occurred in *pod1* mutant

(Figure 2a). In addition, some flowers of *SlMED18* silenced lines showed homeotic alterations in the second and the third floral organ whorls similar to those observed in *pod1* flowers (Figure S3). Likewise, a small amount of non-viable pollen grains was developed from *SlMED18* repressed lines (Figure 2b). Regarding the fruits, there was a strong similarity among RNAi *SlMED18*, double RNAi and *pod1* plants, as all of them yielded parthenocarpic fruits with a decreased fresh weight (Figure 2c). On the contrary, RNAi *ZNHIT* transgenic plants displayed a similar phenotype to WT plants with no obvious alteration in reproductive developmental traits (Figure 2a-c). Moreover, offsprings of RNAi *ZNHIT* lines also showed a WT phenotype, supporting the hypothesis that *pod1* mutant phenotype was caused by the loss of function of *SlMED18*.

To further confirm that down-regulation of *SlMED18* is responsible for the *pod1* phenotype, a molecular complementation assay was performed by overexpressing *SlMED18* in *pod1* plants under the control of a 35S constitutive promoter. Reproductive development of 35S::*SlMED18 pod1* lines were similar to WT controls (Figure 2a-c; Table S1), indicating that the overexpression of *SlMED18* gene was able to rescue the *pod1* mutant phenotype.

Expression patterns of *SlMED18* during tomato reproductive development
SlMED18 is expressed from floral buds to mature fruits, although the highest level of *SlMED18* transcripts was detected in flowers at anthesis, and the lowest one was found in fruits at immature green stage (Figure 3a). *In situ* hybridization analysis of *SlMED18* in developing flower buds showed that *SlMED18* mRNA was located in the two inner whorls of floral buds at stage 5 (according to Brukhin *et al*., 2003), where stamen and carpel primordia were initiated (Figure 3b,c). Later, expression of *SlMED18* was strongly detectable in pollen and ovules at stage 8 of flower development (Figure 3d). Additionally, as the binary vector pD991 used for generating the enhancer trap lines contained a minimal promoter fused to the *uidA* reporter gene, a histochemical GUS assay was performed assuming that *GUS* expression is due to the activity of endogenous regulatory elements that promote the transcription of the *uidA* gene. In *pod1* flowers, GUS staining was detected in stamens, stigma and ovules (Figure 3e), supporting that *SlMED18* gene is specifically expressed in the two innermost floral organs.

In addition, given the homeotic conversion of stamens into carpel organs found in a low number of *pod1* flowers, expression of *SlMED18* was analysed in the floral organs developed in the third whorl of *pod1* mutant flowers. All *pod1* mutant flowers

showed down-regulation of *SlMED18* regardless of the existence of stamen to carpel homeotic conversion (Figure S1g), suggesting that such developmental alterations may correspond to pleiotropic effects of *pod1* mutation rather than being a direct consequence of the loss of *SlMED18* function.

Down-regulation of *SlMED18* affects microgametogenesis and tapetum degradation

Flowers of *pod1* and *SlMED18* silenced lines developed a small proportion of viable pollen (Figure 2b); thus, a detailed study at the cellular level was performed to detect changes in pollen ontogeny promoted by the down-regulation of *SlMED18* function (Figure 4). To rule out any effect of *ZNHIT* down-regulation, RNAi *SlMED18* lines were used for this study instead of *pod1* mutant. PMCs prior to meiosis did not differ in their morphological features when observed in thin tissue sections. Indeed, the characteristic polyhedral shape, slightly stained cytoplasm, and visible nuclei with densely stained nucleolus were observed both in WT and RNAi *SlMED18* plants (Figure 4a,d). Meiocytes at telophase I stage were also similar in shape, size and cytological characters, as well as the features of callose layer, and cytoplasm and chromatin staining properties (Figure 4b,e). These results pointed out to an equally canonical meiosis occurring during pollen development of the *SlMED18* silenced plants. Callose-embraced microspores within the tetrad also showed no differences between both WT and silenced lines, thus, tetrad walls appear well defined and microspores show stained nuclei with nucleoli (Figure 4c,f). Moreover, at meiocyte and tetrad stages no appreciable differences were detected in the size and morphological features of the tapetum and the remaining layers of the anther wall (Figure 4a-f).

Subsequent stages of pollen development were also analysed and DAPI staining of squashed anther samples was performed in order to assess the corresponding microgametogenesis stage engaged, based on the presence and the position of nuclei. Vacuolated microspores showed a typical cytoplasmic distribution in WT anthers, with the occurrence of cytoplasmic vacuoles and a single nucleus clearly stained by DAPI (Figure 4g,j). However, RNAi *SlMED18* flowers developed some microspores which were smaller in size and displayed lower DAPI staining (Figure 4m,p), likely reflecting symptoms of chromatin disorganization. Differences between the WT and the RNAi *SlMED18* plants increased at the stages of young and mature pollen, with a progressive larger proportion of pollen grains with altered morphology, mainly small size,

differential cytoplasmic density, and the presence of empty pollen grains (Figure 4h,i,n,o). DAPI staining analysis of RNAi *SlMED18* anthers showed a reduced amount of apparently normal pollen grains with both the vegetative and the generative nuclei. Instead, a higher proportion of abnormal pollen grains either bearing degenerated nuclei or completely lacking nuclei were observed in anthers where *SlMED18* was silenced (Figure 4k,l,q,r).

Developmental differences in the timing and completion of tapetum degeneration were found throughout microgametogenesis of WT and RNAi *SlMED18* anthers (Figure 5). Although histological features and relative size of the tapetum layer until the tetrad stage were identical in both types of plants, the subsequent tapetal degeneration that begins at the microspore stage in the WT plants (Figure 5a-c) was delayed in *SlMED18* silenced plants (Figure 5d-f). Indeed, while tapetum tissue showed evident degradation symptoms and had almost disappeared at mature pollen stage in WT anthers (Figure 5c), it remains intact in RNAi plants (Figure 5f,g). Taken together, these observations indicated that the lack of *SlMED18* function provoked significant changes during pollen ontogeny, which affected mainly tapetum degradation and pollen maturation. Such developmental abnormalities correlated with the lower percentage of pollen yielded by RNAi *SlMED18* plants.

Silencing of *SlMED18* modifies expression of genes involved in anther and pollen development

To investigate how the lack of *SlMED18* affects the expression of genes involved in anther and pollen ontogeny, a comparative qRT-PCR analysis was carried out in floral buds at five pivotal stages of anther development, i.e. PMCs, tetrads (Tds), young and vacuolated microspores (Mcs), young pollen (YP) and mature pollen (MP) (Figure 6). Thereby, the expression pattern of *SlMED18* and seventeen additional genes previously described as key regulators involved in tomato pollen and anther development was evaluated (Jeong *et al*., 2014, Gómez *et al*., 2015). Given that the asynchrony in the degradation timing of the tapetum suggested an abnormal RNAi *SlMED18* pollen formation, the considered genes were divided into two groups according to their functions in WT anthers: genes related to tapetum degradation and moreover, genes associated to pollen formation and maturation. In addition to *SlMED18*, the first group included *SlSPL/HYDRA*, *MS10[35]*, *AMS-like*, *AtMYB103-like*, *MS1-like*, *TGAS100*, *bHLH89/91, TA29, Cysteine protease*, *Aspartic proteinase* and *Arabinogalactan protein*

10

(Figure 6), while the second one comprised *Sister chromatid cohesion*, *TomA108*, *LeGRP92*, *Endo-1,3-beta-glucanase*, *AtTDF1-like* and *pLAT52* (Figure S4). Most of the tapetum development related genes here analysed were down-regulated at some stage of pollen development in RNAi *SlMED18* lines (Figure 6c-f,i-l). However, *SlSPL/HYDRA* and *bHLH89/91* were expressed without significant differences between WT and RNAi *SlMED18* anthers in all stages analysed (Figure 6b,h). In the case of *TGAS100*, the relative expression was up-regulated at PMCs stage, while it was down-regulated at YP stage (Figure 6g).

In the second group, analysed genes were involved in different functions linked to pollen formation (Figure S4), i.e. pollen meiosis (*Sister chromatid cohesion* and *TomA108*), callose degradation (*Endo-1,3-beta-glucanase* and *AtTDF1-like*), exine formation (*LeGRP92*) and pollen germination (*pLAT52*). All these genes showed significant down-regulation in RNAi *SlMED18* lines, except for *Sister chromatid cohesion*, which was up-regulated at PMC stage and down-regulated at Tds and MP stages (Figure S4a). Considering the alterations in gene expression due to the silencing of *SlMED18*, altogether these results showed that the lack of *SlMED18* function promoted a significant down-regulation of genes mainly related to anther and pollen development, which correlated with the defects observed in tapetum and pollen formation.

SlMED18 complements the phenotypic defects of Arabidopsis *med18-1* mutant

In Arabidopsis, mutations at the *MEDIATOR SUBUNIT 18* (*AtMED18*) cause pleiotropic phenotypic alterations affecting inflorescence structure, flower morphology, silique size, and flowering time (Figure 7a-d), indicating an essential role for *AtMED18* in the control of these developmental processes. Besides, Arabidopsis *med18* plants also showed alterations in stamen development and pollen maturation (Zheng *et al*., 2013). To assess whether *SlMED18* could complement the developmental defects observed in *med18-1* mutants, several Arabidopsis transgenic plants overexpressing the tomato *MED18* orthologue were generated by using a 35S constitutive promoter (Figure 7, Figure S5a). Under long-day conditions, *med18-1* mutants displayed a late flowering phenotype that was fully rescued by the overexpression of *SlMED18* (Figure 7a,d,e). Indeed, expression of *FLOWERING LOCUS T* (*FT*), *SUPPRESSOR OF CONSTANS OVEREXPRESSION 1* (*SOC1*) and *FLOWERING LOCUS C* (*FLC*) genes was restored to similar transcriptional levels, or even higher than those showed by WT plants (Figure

11

S5b). Furthermore, the altered floral organ number and the decreased silique size observed in *med18-1* were complemented by the expression of tomato *MED18* orthologue in the Arabidopsis mutant (Figure 7b,c,f). Thus, flower identity genes such as *SEPALLATA 3* (*SEP3*), *PISTILLATA* (*PI*) and *AGAMOUS* (*AG*), which were down-regulated in Arabidopsis *med18-1* mutant flowers, showed transcriptional levels similar to WT when *SlMED18* was over-expressed in *med18-1* plants (Figure S5c). These results indicated that *SlMED18* fulfil the functional roles exerted by the Arabidopsis *MED18* gene.

DISCUSSION

Transcriptional activity of *SlMED18* is essential for tapetum degradation and pollen development

The *pod1* tomato T-DNA mutant is severely affected in flower and pollen development. Molecular cloning of the tagged gene proved that *POD1* encodes the Mediator of RNA polymerase II transcription subunit 18 (MED18) supporting a functional role for this gene in reproductive development of tomato. GUS expression was detected in the stigma and pollen sacs (Figure 3e), which agrees with the spatial expression pattern detected by *in situ* hybridization (Figure 3c,d). These results support that transcriptional activity of *SlMED18* is required during male gametogenesis. Although no morphological alterations were observed at early stages of pollen development of plants lacking *POD1/SlMED18*, microscopy analysis revealed changes during microgametogenesis (Figure 4), which involved a significant delay in tapetum degeneration as compared to WT (Figure 5). Moreover, from microspore stage onwards, defective anthers yielded a low amount of mature pollen grains, most of them being degenerated cells (near to 83%). Adequate sporophytic cell layer development is necessary to give rise to functional mature pollen in plants (Ma, 2005; Yuan *et al*., 2009; Zhou *et al*., 2011), being the tapetum the most important layer, since it supplies nutrients required for pollen development. Indeed, male sterility is normally associated with abnormal tapetum development, as occurs in the Arabidopsis *ems1/exs* and *tpd1* mutants (Canales *et al*., 2002; Zhao *et al*., 2002; Yang *et al*., 2003), as well as in the tomato mutants affected either in *SlCER6* or *Ms10³⁵* genes (Smirnova *et al*., 2013; Jeong *et al*., 2014). All of these mutants showed early tapetum degradation, the opposite effect to that observed in RNAi *SlMED18* plants where tapetum degenerated later than in WT plants. However, the consequence in both cases was an abnormal pollen

formation, which corroborates that timely coordinated degradation of the tapetum is a crucial step during microgametogenesis, and that this process requires the *SlMED18* function. Therefore, *SlMED18* may act as a link between sporophytic (tapetum tissue) and gametophytic (pollen development) tissues, an hypothesis that would be in agreement with the expression pattern of *SlMED18,* whose transcript levels were mainly found in anther primordia and pollen grains.

Recently, a genetic pathway including *DYT1-TDF1-AMS-bHLH89/91-MYB80* transcriptional cascade has been proposed to regulate tapetum ontogeny in Arabidopsis (Li *et al*., 2017). In addition, *MS10[35]*, the tomato *DYT1* homologue, has been suggested as an upstream regulator of that transcriptional cascade, whose function is necessary for proper meiosis and tapetum development (Jeong *et al*., 2014). *MS10[35]* was significantly repressed in RNAi *SlMED18* anthers suggesting that *SlMED18* may promote tapetum development and degradation through direct or indirect regulation of *MS10[35]*. In accordance with this, several tapetum development-related genes were down-regulated in RNAi *SlMED18* plants as occurred with *AtTDF1-like*, *AMS*-like, *Cysteine protease*, *Aspartic proteinase*, *TA29* and *MS1-like*, which support that tapetum functionality should be compromised by the lack of *SlMED18*.

Together, the results reported here provide strong evidence about the function of *SlMED18* in the transcriptional regulation of a subset of genes specifically required to develop mature pollen properly. In addition, hormones play a central role in male gametogenesis, and the function of *SlMED18* in the modulation of genes involved in hormonal pathways cannot be ruled out. Nevertheless, further research is required to better understand the hierarchical and functional relationships among the genes integrating the regulatory pathway involved in pollen development and their link with hormone pathways.

Functional divergence of *SlMED18* gene

The Mediator complex is recognised as a central player in eukaryotic gene regulation. In Arabidopsis, several functions have been reported for the different subunits integrating this complex (Zheng *et al*., 2013; Samanta and Thakur, 2015; Fallath *et al*., 2017). Although such functions must be interconnected, subunits that integrate the same Mediator module seem to participate in the same biological process (Davoine *et al*., 2017). *MED18* belongs to the head-module Mediator complex that was originally identified as a general transcription factor that stimulates basal RNA Polymerase II

transcription in yeast (Kornberg, 2005; Larivière *et al.*, 2006). Later, yeast *MED18* was described as a key element for proper elongation (Lee *et al.*, 2013) and termination of transcription of a subset of genes (Mukundan and Ansari, 2011). In Arabidopsis, it has been proposed that *MED18* regulates flowering time and floral organ formation through regulation of *FLC* and *AG*, respectively (Zheng *et al.*, 2013). Expression levels of the floral repressor *FLC* were found up-regulated in *med18-1* plants, which also agreed with the late flowering phenotype of these mutants. Concomitantly, decreased expression of *FT* and *SOC1* floral integrators were detected in *med18* (Zheng *et al.*, 2013). In addition, the number of petals increased and the number of stamens decreased in *med18* plants, two features which were reminiscent of the floral phenotype of *ag* mutants (Chuang and Meyerowitz, 2000). In accordance, epistasis was observed in the *med18-1 ag-1* double mutants and *AG* expression was down-regulated in *med18-1* plants (Zheng *et al.*, 2013). Interestingly, constitutive expression of *SlMED18* in Arabidopsis *med18* background rescues all the developmental defects displayed by *med18-1* plants related to flowering time and floral organ identity. Furthermore, *SlMED18* also complements the altered pattern of expression of the key genes involved in the regulation of these processes (Figure S5). Thus, expression levels of *AG*, *PI* and *SEP3* increased in complemented *med18* plants, supporting that the *MED18* tomato orthologue is able to regulate the expression of these identity genes in Arabidopsis and rescue the defects in flowering time and floral organ number observed in *med18* plants.

Overall results indicated that *SlMED18* shares significant biological function with Arabidopsis *MED18*. In addition to the altered floral organ number, Arabidopsis *med18* mutants also showed a delay both in stamen development and pollen maturation, which led to a reduction in seed set (Zhang *et al.*, 2013). These results indicate that *MED18* is also involved in the genetic control of male gametogenesis for this model species; although a detailed study of pollen ontogeny, similar to that conducted here with tomato, would be necessary in Arabidopsis to draw a final conclusion on the maintenance or divergence of MED18 function in these species. Nevertheless, in contrast to Arabidopsis *med18* mutants, *pod1* plants and *SlMED18* silenced lines showed no alterations in flowering time and reduced penetrance and variable expressivity of floral homeotic changes. As described for the Arabidopsis *med18* mutant, the occasional homeotic changes observed in the third floral whorl of *pod1* and RNAi *SlMED18* plants could be the consequence of the down-regulation of the tomato B-class identity key genes *TPI*, *TM6* and *SL* (Figure S1g). Altogether, these

14

observations suggest certain functional divergence between tomato and Arabidopsis MED18 orthologues. Interestingly, a single *MED18* gene has been found in the Arabidopsis genome (*AT2G22370*), whereas in tomato two paralogous *MED18* genes have been annotated (i.e, *Solyc03g046360* and *Solyc03g046370*) apart from the orthologous *SlMED18* gene (*Solyc06g008020*) reported here (Figure S6), indicating a different evolution dynamics for this family gene in these species.

Experimental procedures

Plant material

Tomato *pod1* mutant was isolated from a collection of T-DNA insertion lines generated by the enhancer trap vector pD991 in the tomato cv. Moneymaker (Pérez-Martín *et al*., 2017). All tomato plants were grown under greenhouse conditions using standard practices with regular addition of fertilizers. The *med18-1* mutant in Columbia (Col) genetic background was kindly provided by Dr. David Oppenheimer (Zheng *et al*., 2013).

Histochemical GUS staining

A GUS assay was carried out following the method described by Atarés *et al*. (2011). The resulting GUS-stained tissues were examined under a zoom stereomicroscope (MZFLIII, Leica). Three replicates of each sample were analysed.

Analysis of pollen viability

In vitro pollen viability was determined by the Tetrazolium staining method (Cottrell, 1948). Pollen grains from more than 30 flowers of each genotype were stained with 0.5% 2, 3, 5-triphenil tetrazolium chloride (TTC) (w/v) in 0.5 M sucrose in a wet chamber for 2h at 50°C in darkness (Viéitez Cortizo, 1952). Subsequently, pollen was visualised with a Nikon OPTIPHOT-2 optical microscope.

To evaluate *in vivo* pollen viability the Johansen´s (1940) staining method for fluorescence microscope was assayed. Ten flowers from each WT and *pod1* plants were self-pollinated and reciprocally crossed. Two days after pollination, these flowers were collected and fixed in FAE (10% formaldehyde, 5% acetic acid and 50% absolute ethanol) for at least 24h, washed in water over night at 4°C, softened with NaOH 0.8 N during 6h and washed again in water over night at 4°C. Pollen tubes were stained with 0.1% aniline blue (w/v) in K_3PO_4 0.1 N for 2h in darkness. Fluorescence was visualised

with a Nikon OPTIPHOT-2 optical microscope associated to HB-10101AF Mercury Lamp (Nikon).

Molecular cloning procedures

The DNA-blot hybridization was carried out following the protocol described by Yuste-Lisbona *et al*. (2016). Hybridization was performed with a chimeric probe constituted by the fused coding sequence of two genes, *NEOMYCIN PHOSPHOTRANSFERASE II* (*NPTII*) and *FALSIFLORA* (*FA*), the later was used as hybridization positive control.

The sequences flanking T-DNA insertion sites were isolated by a modified anchor-PCR according to the protocol described by Pérez-Martín *et al*. (2017). The cloned sequences were compared with SGN Database (http://solgenomics.net/) to assign the T-DNA insertion site on tomato genome.

Co-segregation of the T-DNA insertion site with the *pod1* phenotype was evaluated by PCR using i) the specific genomic forward and reverse primers (619a_genot_F/_R) to amplify the WT allele (without T-DNA insertion) and ii) one specific genomic primer (619a_genot_R) and the specific T-DNA right border primer (RB_pD991_F) to amplify the mutant allele (carrying the T-DNA insertion). The sequences of anchor-PCR and genotyping primers used are listed in Table S2.

Generation of transgenic lines

An interference RNA (RNAi) approach was performed to down-regulate candidate genes. To generate the RNAi *SlMED18* construct, a 164 bp fragment of *SlMED18* cDNA was cloned in sense and antisense orientation into the vector pKannibal (Wesley *et al*., 2001), which was digested with *Not*I and the resulting fragment was cloned into the binary vector pART27 (Gleave, 1992) following the method described by Helliwell and Waterhouse (2003). Likewise, a 248 bp fragment of the *ZNHIT* cDNA was used to generate the RNAi *ZNHIT* construct. In addition, both *SlMED18* and *ZNHIT* genes were simultaneously inhibited by a double RNAi construct. For this purpose, the 164 bp fragment of *SlMED18* was amplified using RNAi-doble_F and RNAiMED18_R primers, and the RNAiZn_F and RNAi-doble_R primers were used to amplify the 248 bp fragment of the *ZNHIT* gene. Thereupon, both fragments were used as template in a PCR using the primers RNAiZn_F and RNAiMED18_R to join the PCR products resulting from the above PCR amplifications. The resulting PCR product was finally cloned in pART27 as described above.

16

To generate the overexpression gene construct (35S::*SlMED18*), the complete open reading frame of *SlMED18* was amplified from *S. lycopersicum* cv. Moneymaker cDNA using 35S-Med_F and 35S-Med_R primers. The *SlMED18* cDNA was cloned into the binary vector pROKII (Baulcombe *et al*., 1986). The overexpression construct 35S::*SlMED18* was also used for genetic complementation of *pod1* plants. The sequences of primers used in the generation of silencing and overexpression constructs are shown in Table S2.

Genetic transformation experiments were performed using *A. tumefaciens* (strain LBA4404) as described by Ellul *et al*. (2003). The ploidy levels in transgenic plants were evaluated by flow cytometry according to the protocol described by Atarés *et al*. (2011). Thus, diploid RNAi *SlMED18* (6 lines), RNAi *ZNHIT* (5 lines), double RNAi (3 lines) and 35S::*SlMED18* (3 lines) transgenic plants were selected for further phenotypic and expression analyses.

Microscopy analysis

Anther sections at key stages of microsporogenesis in the WT and transgenic genotypes were processed for light microscopy according to Jimenez-Lopez *et al*. (2016). Sections (7 μm) were stained with a mix of toluidine blue/methylene blue, and observed in a Nikon Eclipse Ti-U microscope.

For the study of nuclei, pollen grains were released on a slide by squash from at least 20 anthers at four different stages and stained with 4´,6´-diamidino-2-phenylindole (10 ng·ml^{-1}, DAPI) in McIlvaine buffer (0.1 M citric acid, 0.2 M Na_2HPO_4, 1% Triton X-100, pH 4.0) according to the method previously described by Coleman and Goff (1985). Samples were incubated at room temperature for 15 min in darkness and examined using using an epifluorescence microscope Nikon OPTIPHOT-2 associated to HB-10101AF Mercury Lamp (Nikon).

Scanning electron microscopy (SEM) analyses were carried out as previously described by Lozano *et al*. (1998). Flowers from *pod1* mutant and WT were fixed in FAEG (10% formaldehyde, 5% acetic acid, 50% absolute ethanol and 0.72% glutaraldehyde) and stored in 70% ethanol. Critical point dried with liquid CO_2 in a critical point drier Bal Tec (Liechtenstein) CPD 030 was performed after dehydration of samples. Gold coat was applied in a Sputter Coater (Bal Tec SCD005). Samples were visualised using the scanning electron microscopy Hitachi S-3500N at 10kV.

Gene expression analysis

Total RNA was isolated using TRIZOL (Invitrogen) following the manufacturer's instructions from flowers at 5 different stages in relation to pollen cells development: PMCs (floral buds of 1-2 mm); Tds (floral buds of 3-4 mm); Mcs (flowers of 5-6 mm); YP (flowers of 7-8 mm); and MP (flowers at anthesis). cDNA was synthesized from 500 ng of total RNA using the M-MuLV reverse transcriptase (Fermentas Life Sciences) with a mixture of random hexamer and oligo(dT)$_{18}$ primers. Expression analyses were performed with three biological and two technical replicates. qRT-PCRs were performed with the SYBR Green PCR Master Mix (Applied Biosystems) kit using the 7300 Real-Time PCR System (Applied Biosystems). The housekeeping *Ubiquitine3* gene was used as control in all gene expression analyses. Specific primer pairs for each evaluated gene were described in Table S3. Results were expressed using the ΔΔCt calculation method (Winer *et al*., 1999) in arbitrary units by comparison with a data point from the WT samples.

In situ hybridization assays, tissue preparation, sectioning and transcript detection were carried out as described by Lozano *et al.* (1998). A *POD1/SlMED18* probe was prepared using cDNA as template (200-pb fragment of the 3'UTR from the *Solyc06g008010* gene). Antisense probe was synthesized using the DIG RNA labelling mix (Roche Applied Science). As negative control, sense RNA probe was hybridized with the same sections and no signals were observed under the hybridization and detection conditions used.

Genetic complementation of the Arabidopsis *med18-1* mutant

The overexpression construct 35S::*SlMED18* was transformed in the Arabidopsis *med18-1* plants (Zheng *et al*., 2013) by *A. tumefaciens* (strain C58C1) mediated transformation using the floral-dip method (Clough and Bent, 1998). The resulting 35S::*SlMED18 med18-1* transgenic lines were selected on MS-glucose kanamycin-containing media plates. At least 10 independent transformants were evaluated phenotypically for different reproductive traits.

Controlled environmental conditions were provided by walk-in growth chambers at 22ºC and 65% relative humidity. For the *in vitro* experiments, seedlings were cultured on agar-solidified MS medium. Plants were illuminated with cool-white fluorescent lights (120 μmoles/m^2/s); Long-day (LD) conditions consisted of 16h light/8h dark and short-day (SD) conditions were 8h light/16h dark.

Acknowledgements

Conflict of interest

The author(s) declare that they have no competing interests

Supporting information

Figure S1. Scanning electron microscopy analysis and expression of B- and C-class genes in wild-type and *pod1* plants.

Figure S2. Relative expression of *SlMED18* and *ZNHIT* genes in transgenic lines.

Figure S3. Floral homeotic changes displayed by *pod1* mutants and *SlMED18* silenced lines.

Figure S4. Relative expression of pollen marker genes in floral buds of wild-type (WT) and RNAi *SlMED18* plants.

Figure S5. Relative expression levels of flowering time and floral organ identity genes are restored in 35S::*SlMED18 med18-1* plants of *Arabidopsis thaliana.*

Figure S6. Phylogenetic analysis of *MED18* homologue genes.

Table S1. Relevant phenotypic traits measured in the wild-type, *pod1* mutant, and transgenic lines.

Table S2. Primer sequences used for anchor-PCR, genotyping and transgenic constructs

Table S3. Primer sequences used for qRT-PCR analyses

References

Allen, B.L. and Taatjes, D.J. (2015). The Mediator complex: a central integrator of transcription. *Nat. Rev. Mol. Cell Biol.* **16**, 155-166.

Atarés, A., Moyano, E., Morales, B., Schleicher, P., García-Abellán, J.O., Antón, T., García-Sogo, B., *et al.* (2011). An insertional mutagenesis programme with an enhancer trap for the identification and tagging of genes involved in abiotic

stress tolerance in the tomato wild-related species *Solanum pennellii. Plant Cell Rep.* **30**, 1865-1879.

Baulcombe, D.C. (1986). Mechanisms of Pathogen-Derived Resistance to Viruses in Transgenic Plants. *Plant Cell* **8**, 1833-1844.

Bourbon, H.M. (2008). Comparative genomics supports a deep evolutionary origin for the large four-module transcriptional mediator complex. *Nucleic Acids Res.* **36**, 3993-4008.

Brukhin, V., Hernould, M., Gonzalez, N., Chevalier, C. and Mouras, A. (2003). Flower development schedule in tomato *Lycopersicon esculentum* cv. sweet cherry. *Sex Plant Rep.* **15**, 311-320.

Buendía-Monreal, M. and Gillmor, C.S. (2016). Mediator: A key regulator of plant development. *Dev. Biol.* **419**, 7-18.

Canales, C., Bhatt, A.M., Scott, R. and Dickinson, H. (2002). *EXS*, a putative *LRR* receptor kinase, regulates male germline cell number and tapetal identity and promotes seed development in Arabidopsis. *Curr. Biol.* **12**, 1718-1727.

Carbonell-Bejerano, P., Urbez, C., Carbonell, J., Granell, A. and Perez-Amador, M.A. (2010). A fertilization-independent developmental program triggers partial fruit development and senescence processes in pistils of Arabidopsis. *Plant Physiol.* **154**, 163-172.

Chadick, J.Z. and Asturias, F.J. (2005). Structure of eukaryotic Mediator complexes. *Trends Biochem. Sci.* **30**, 264-271.

Chuang, C.F. and Meyerowitz, E.M. (2000). Specific and heritable genetic interference by double-stranded RNA in *Arabidopsis thaliana. Proc. Natl. Acad. Sci. USA* **97**, 4985-4990.

Clough, S.J. and Bent, A.F. (1998). Floral dip: a simplified method for *Agrobacterium*-mediated transformation of *Arabidopsis thaliana. Plant J.* **16**, 735-743.

Coleman, A.W. and Goff, L.J. (1985). Applications of fluorochromes to pollen biology. I. Mithramycin and 4',6-diamidino-2-phenylindole (DAPI) as vital stains and for quantitation of nuclear DNA. *Stain Technol.* **60**, 145-154.

Conaway, R.C., Sato, S., Tomomori-Sato, C., Yao, T. and Conaway, J.W., (2005). The mammalian Mediator complex and its role in transcriptional regulation. *Trends Biochem. Sci.* **30**, 250-255.

Cottrell, H. J. (1948). Tetrazolium salt as a seed germination indicator. *Ann. Appl. Biol*. **35**, 123-131.

Crane, M.B. (1915). Heredity of types of inflorescence and fruits in tomato. *J. Genet.* **5**, 1-11.

Davoine, C., Abreu, I.N., Khajeh, K., Blomberg, J., Kidd, B.N., Kazan, K., Schenk, P.M., *et al.* (2017). Functional metabolomics as a tool to analyze Mediator function and structure in plants. *PLoS ONE* **12**, e0179640.

Ellul, P., García-Sogo, B., Pineda, B., Ríos, G., Roig, L.A. and Moreno, V. (2003). The ploidy level of transgenic plants in Agrobacterium-mediated transformation of tomato cotyledons (*Lycopersicon esculentum* L. Mill.) is genotype and procedure dependent. *Theor. Appl. Genet.* **106**, 231-238.

Fallath, T., Kidd, B.N., Stiller, J., Davoine, C., Björklund, S., Manners, J.M., Kazan, K. *et al*. (2017). *MEDIATOR18* and *MEDIATOR20* confer susceptibility to *Fusarium oxysporum* in *Arabidopsis thaliana*. *PLoS ONE* **12**, e0176022.

Feng, B., Lu, D., Ma, X., Peng, Y., Sun, Y., Ning, G. and Ma, H. (2012). Regulation of the Arabidopsis anther transcriptome by *DYT1* for pollen development. *Plant J.* **72**, 612-624.

Gillaspy, G., Ben-David, H. and Gruissem, W. (1993). Fruits: a developmental perspective. *Plant Cell* **5**, 1439-1451.

Gleave, A.P. (1992). A versatile binary vector system with a T-DNA organisational structure conducive to efficient integration of cloned DNA into the plant genome. *Plant Mol Biol.* **20**, 1203-1207.

Gómez, J.F., Talle, B. and Wilson, Z.A. (2015). Anther and pollen development: a conserved developmental pathway. *J. Integr. Plant Biol.* **57**, 876-891.

Gorman, S.W. and McCormick, S. (1997). Male sterility in tomato. *Crit. Rev. Plant Sci.* **16**, 31-53.

Helliwell, C. and Waterhouse, P. (2003). Constructs and methods for high-throughput gene silencing in plants. *Methods* **30**, 289-295.

Honys, D. and Twell, D. (2004). Transcriptome analysis of haploid male gametophyte development in Arabidopsis. *Genome Biol.* **5**, R85.

Jeong, H.J., Kang, J.H., Zhao, M., Kwon, J.K., Choi, H.S., Bae, J.H., Lee, H.A., *et al*. (2014). Tomato *Male sterile 10³⁵* is essential for pollen development and meiosis in anthers. *J. Exp. Bot.* **65**, 6693-6709.

Jimenez-Lopez, J.C., Zienkiewicz, A., Zienkiewicz, K., Alché, J.D. and Rodríguez-García, M.I. (2016). Biogenesis of protein bodies during legumin accumulation in developing olive (*Olea europaea* L.) seed. *Protoplasma* **253**, 517-530.

Johansen, D. A. (1940). *Plant microtechniques*. McGraw-Hill Book Co., New York, USA. ISBN: 978-0070325401.

Kornberg, R.D. (2005). Mediator and the mechanism of transcriptional activation. *Trends Biochem. Sci.* **30**, 235-239.

Lai, Z., Schluttenhofer, C.M., Bhide, K., Shreve, J., Thimmapuram, J., Lee, S.Y., Yun, D.J. *et al*. (2014). *MED18* interaction with distinct transcription factors regulates multiple plant functions. *Nat. Commun.* **5**, 3064.

Larivière, L., Geiger, S., Hoeppner, S., Röther, S., Strässer, K. and Cramer, P. (2006). Structure and TBP binding of the Mediator head subcomplex Med8-Med18-Med20. *Nat. Struct. Mol. Biol.* **13**, 895-901.

Lee, S.K., Chen, X., Huang, L. and Stargell, L.A. (2013). The head module of Mediator directs activation of preloaded RNAPII *in vivo*. *Nucleic Acids Res.* **41**, 10124-10134.

Li, D.D., Xue, J.S., Zhu, J. and Yang Z.N. (2017). Gene Regulatory Network for Tapetum Development in *Arabidopsis thaliana*. *Front. Plant Sci.* **8**, 1559.

Liu, X., Huang, J., Parameswaran, S., Ito, T., Seubert, B., Auer, M., Rymaszewski, A., *et al*. (2009). The *SPOROCYTELESS/NOZZLE* gene is involved in controlling stamen identity in Arabidopsis. *Plant Physiol.* **151**, 1401-1411.

Lora, J., Hormaza, J.I., Herrero, M. and Gasser, C.S. (2011). Seedless fruits and the disruption of a conserved genetic pathway in angiosperm ovule development. *Proc. Natl. Acad. Sci. USA* **108**, 5461-5465.

Lozano, R., Angosto, T., Gómez, P., Payán, C., Capel, J., Huijser, P., Salinas, J. *et al*. (1998). Tomato flower abnormalities induced by low temperatures are associated with changes of expression of MADS-box genes. *Plant Physiol.* **117**, 91-100.

Ma, H. (2005). Molecular genetic analyses of microsporogenesis and microgametogenesis in flowering plants. *Ann. Rev. Plant Biol.* **56**, 393-434.

McNeil, K.J. and Smith, A.G. (2010). A glycine-rich protein that facilitates exine formation during tomato pollen development. *Planta* **231**, 793–808.

Mercier, R., Armstrong, S.J., Horlow, C., Jackson, N.P., Makaroff, C.A., Vezon, D., Pelletier, G., *et al*. (2003). The meiotic protein SWI1 is required for axial element formation and recombination initiation in Arabidopsis. *Development* **130**, 3309-3318.

Mukundan, B. and Ansari, A. (2011). Novel role for mediator complex subunit Srb5/Med18 in termination of transcription. *Biol. Chem.* **286**, 37053-37057.

Muschietti, J., Dircks, L., Vancanneyt, G. and McCormick, S. (1994). LAT52 protein is essential for tomato pollen development: Pollen expressing antisense LAT52 RNA hydrates and germinates abnormally and cannot achieve fertilization. *Plant J.* **6**, 321-338.

Ozga, J.A. and Reinecke, D.M. (2003). Hormonal interactions in fruit development. *J. Plant Growth Regul.* **22**, 73-81.

Pacini, E. (2010) Relationships between tapetum, loculus and pollen during development. *Int. J. Plant Sci.* **171**, 1-11.

Pérez-Martín, F., Yuste-Lisbona, F.J., Pineda, B., Angarita-Díaz, M.P., García-Sogo, B., Antón, T., Sánchez, S., *et al.* (2017). A collection of enhancer trap insertional mutants for functional genomics in tomato. *Plant Biotech. J.* **15**, 1439-1452.

Pina, C., Pinto, F., Feijó, J.A. and Becker, J.D. (2005). Gene family analysis of the Arabidopsis pollen transcriptome reveals biological implications for cell growth, division control, and gene expression regulation. *Plant Physiol.* **138**, 744-756.

Polowick, P.L. and Sawhney, C.K. (1993a). An ultrastructural study of pollen development in tomato (*Lycopersicon esculentum*) I. Tetrad to early binucleate microspore stage. *Can. J. Bot.* **71**, 1039-1047.

Polowick, P. L. and Sawhney, C. K. (1993b). An ultrastructural study of pollen development in tomato (*Lycopersicon esculentum*) II. Pollen maturation. *Can. J. Bot.* **71**, 1048-1055.

Rutley, N. and Twell, D. (2015). A decade of pollen transcriptomics. *Plant Reprod.* **28**, 73-89.

Samanta, S. and Thakur, J.K. (2015). Importance of Mediator complex in the regulation and integration of diverse signaling pathways in plants. *Front. Plant Sci.* **6**, 757.

Schiefthaler, U., Balasubramanian, S., Sieber, P., Chevalier, D., Wisman, E. and Schneitz, K. (1999). Molecular analysis of *NOZZLE*, a gene involved in pattern formation and early sporogenesis during sex organ development in *Arabidopsis thaliana*. *Proc. Natl. Acad. Sci. USA* **96**, 11664-11669.

Scott, R.J., Spielman, M. and Dickinson, H.G. (2004). Stamen structure and function. *Plant Cell* **16**, S46–S60.

Smirnova, A., Leide, J. and Riederer, M. (2013). Deficiency in a very-long-chain fatty acid β-ketoacyl-coenzyme a synthase of tomato impairs microgametogenesis and causes floral organ fusion. *Plant Physiol.* **161**, 196-209.

Sorensen, A.M., Krober, S., Unte, U.S., Huijser, P., Dekker, K. and Saedler, H. (2003). The Arabidopsis *ABORTED MICROSPORES* (*AMS*) gene encodes a *MYC* class transcription factor. *Plant J.* **33**, 413-423.

Viéitez Cortizo, E. (1952). El uso del cloruro 2, 3, 5-trifeniltetrazolium para determinar la vitalidad del polen. In: *Anales de edafología y fisiología vegetal* (ed. Consejo Superior de Investigaciones Científicas), pp. 1033-1044. Madrid: Digital. CSIC.

Wang, Y., Hu, Z., Zhang, J., Yu, X, Guo, J.E., Liang, H., Liao, C., *et al.* (2018) Silencing *SlMED18*, tomato Mediator subunit 18 gene, restricts internode elongation and leaf expansion. *Sci. Rep.* **8**, 3285.

Wesley, S.V., Helliwell, C.A., Smith, N.A., Wang, M.B., Rouse, D.T., Liu, Q., Gooding, P.S., *et al*. (2001). Construct design for efficient, effective and high-throughput gene silencing in plants. *Plant J.* **27**, 581-590.

Wilson, Z.A., Morroll, S.M., Dawson, J., Swarup, R. and Tighe, P.J. (2001). The Arabidopsis *MALE STERILITY1* (*MS1*) gene is a transcriptional regulator of male gametogenesis, with homology to the PHD-finger family of transcription factors. *Plant J.* **28**, 27-39.

Wilson, Z.A. and Zhang, D.B. (2009). From Arabidopsis to rice: pathways in pollen development. *J. Exp. Bot.* **60**, 1479-1492.

Winer, J., Jung, C.K., Shackel, I. and Williams, P.M. (1999). Development and validation of real-time quantitative reverse transcriptase-polymerase chain reaction for monitoring gene expression in cardiac myocytes *in vitro*. *Anal. Biochem.* **15**, 41-49.

Yang, C., Vizcay-Barrena, G., Conner, K. and Wilson, Z.A. (2007). *MALE STERILITY1* is required for tapetal development and pollen wall biosynthesis. *Plant Cell* **19**, 3530-3548.

Yang, C.Y., Spielman, M., Coles, J.P., Li, Y., Ghelani, S., Bourdon, V., Brown, R.C., *et al*. (2003). *TETRASPORE* encodes a kinesin required for male meiotic cytokinesis in Arabidopsis. *Plant J.* **34**, 229-40.

Yang, W.C., Ye, D., Xu, J. and Sundaresan, V. (1999). The *SPOROCYTELESS* gene of Arabidopsis is required for initiation of sporogenesis and encodes a novel nuclear protein. *Genes Dev.* **13**, 2108-2117.

Yuan, W., Li, X., Chang, Y., Wen, R., Chen, G., Zhang, Q. and Wu, C. (2009). Mutation of the rice gene *PAIR3* results in lack of bivalent formation in meiosis. *Plant J.* **59**, 303-315.

Yuste-Lisbona, F.J., Quinet, M., Fernández-Lozano, A., Pineda, B., Moreno, V., Angosto, T. and Lozano, R. (2016). Characterization of *vegetative inflorescence* (*mc-vin*) mutant provides new insight into the role of *MACROCALYX* in regulating inflorescence development of tomato. *Sci. Rep.* **6**, 18796.

Zhao, D.Z., Wang, G.F., Speal, B. and Ma, H. (2002). The *EXCESS MICROSPOROCYTES1* gene encodes a putative leucine-rich repeat receptor protein kinase that controls somatic and reproductive cell fates in the Arabidopsis anther. *Genes Dev.* **16**, 2021-2031.

Zheng, Z., Guan, H., Leal, F., Grey, P.H. and Oppenheimer, D.G. (2013). *Mediator subunit18* controls flowering time and floral organ identity in Arabidopsis. *PLoS ONE* **8**, e53924.

Zhou, S., Wang, Y., Li, W., Zhao, Z., Ren, Y., Wang, Y., Gu, S., *et al*. (2011). *Pollen semi-sterility1* encodes a kinesin-1-like protein important for male meiosis, anther dehiscence, and fertility in rice. *Plant Cell* **23**, 111-129.

Figure legends

Figure 1. Phenotypic and molecular characterization of *pod1* insertional mutant. (a,b) Compared to WT plants (left), both leaf (a) and flower (b) development were reduced in *pod1* plants (right). (c,d) Stamens of WT plants yielded a normal amount of viable pollen stained with TTC (c), while stamens of *pod1* plants produced little amount of viable pollen (d). (e,f) *In vivo* pollen germination analysis. WT pollen grains developed normally on *pod1* stigmas allowing to complete pollination (e), however, *pod1* pollen grains were unable to form pollen tubes on cross-pollinated WT flowers (f). (g) Tomato fruits yielded by *pod1* plants were seedless (parthenocarpic) and displayed a significant reduction in size. Scales bars: 10 cm in (a); 0.5 cm in (b); 200 μm in (c) and (d); 100 μm in (e) and (f); and 1 cm in (g). (h) Southern blot analysis of genomic DNA digested with *Eco*RI (E) and *Hin*dIII (H) and hybridized with a chimeric probe including *NPTII* and *FA* genes (the latter used as hybridization positive control). (i) Genomic organization of the *SlMED18* and *ZNHIT* genes. The T-DNA insertion event produced a 160 bp deletion (Δ_{160}) on the *POD1* genomic region of the mutant. Exons of *SlMED18* and *ZNHIT* are depicted as white and grey boxes, respectively. Promoter region of both genes is shown as a bold line between transcription start sites (ATG). (j) Co-segregation analysis of the T-DNA insertion and the *pod1* mutant phenotype in 16 plants of the T2 population. T2 plants heterozygous (3, 4, 6, 7, 9, 10, 14 and 16) and homozygous for the WT allele (2, 8, 11 and 12) showed WT phenotype, while T2 plants homozygous for the mutant allele (1, 5, 13 and 15) displayed *pod1* mutant phenotype. Dashed circles indicate *pod1* plants displaying mutant phenotype. (k) Quantitative real-time PCR assay for *SlMED18* gene. (l) Quantitative real-time PCR analysis of *ZNHIT* gene. Asterisk denotes significant differences (Student's t-test, $P < 0.05$).

Figure 2. *SlMED18* silencing plants phenocopy the *pod1* mutant phenotype. (a-c) Phenotypic variation of reproductive traits observed in transgenic plants. Morphological features of flowers (a), pollen grains (b) and fruits (c) developed by RNAi *SlMED18* and double RNAi silencing lines were similar to those of *pod1* plants. In contrast, no differences were observed in RNAi *ZNHIT* silencing lines and in *pod1* plants overexpressing *SlMED18* (35S::*SlMED18 pod1*) compared to wild-type (WT) ones. (d) Comparison of the average relative expression of *SlMED18* and *ZNHIT* genes in leaves from WT and transgenic lines. Scale bars: 1 cm in (a) and (c); and 100 μm in (b).

Figure 3. Expression of *SlMED18* in reproductive floral organs. (a) Time-course of *SlMED18* gene expression during flower and fruit development. (b-d) *In situ* hybridization assay of the *SlMED18* gene in tomato flower buds. While no signal was found with sense probe hybridization (b), transcript accumulation signals were found in the two inner whorls of early developed flowers (stage 5, according to Brukhin *et al.*, 2003) (c); later, *SlMED18* transcripts were mainly detected in pollen and ovules in flower buds at stage 8 (d). (e) *GUS* expression was found in stamens, stigma, ovules and at the bottom of petals and carpel of *pod1* flowers, but not in WT ones. S, sepal primordium; P, petal primordium; St, stamen primordium, C, carpel primordium; Ov, ovules; Pg, pollen grains. Scale bars: 100 μm in (b), (c) and (d); and 1 mm in (e).

Figure 4. Microscopy analysis of microsporogenesis and microgametogenesis in wild-type and RNAi *SlMED18* plants. (a-f) Morphological and histological features of anther sections during microsporogenesis of wild-type (a-c) and RNAi *SlMED18* (d-f) plants. No differences were detected at the following developmental stages: pollen mother cells prior to the onset of meiosis (a,d), meiocytes at telophase I stage (b,e), and tetrads (c,f). (g-r) Morphological and histological features of anther sections during microgametogenesis of wild-type (g-l) and RNAi *SlMED18* (m-r) plants; tissue sections were stained either with aniline blue (g-i and m-o) or DAPI (j-l and p-r). Comparative analyses were performed at the following developmental stages: vacuolated microspores (g,j *versus* m,p), young pollen grains (h,k *versus* n,q), and mature pollen grains prior to anther dehiscence (i,l *versus* o,r). Aw, anther wall; Ca, callose; Chr, chromatin; dN, degenerated nucleus; GN, generative nucleus; N, nucleus; PMC, pollen mother cell; T, tapetum; V, vacuole; VN, vegetative nucleus; asterisk, degenerated/altered microspore or pollen grain. Scale bars: 10μm.

Figure 5. Tapetum development is altered during microgametogenesis of RNAi *SlMED18* plants. (a-f) Morphological and histological features of anther sections focused on the tapetal layer at three stages before to anther dehiscence, i.e. vacuolated microspore (a,d), young pollen (b,e) and mature pollen (c,f). (g) Morphometric quantification of the tapetum tissue area (measured as a percentage of the whole anther locule) indicated a higher area of tapetum tissue RNAi *SlMED18* plants. Asterisks

denote significant differences (Student's t-test, $P < 0.05$). Aw, anther wall; T, tapetum. Scale bars: 10μm.

Figure 6. Expression of tapetum marker genes in wild-type and RNAi *SlMED18* plants. qRT-PCR assay for *SlMED18* (a), *SlSPOROCYTLESS/HYDRA* (b), *MS10[35]* (c), *AMS-like* (d), *AtMYB103-like* (e), *MS1*-like (f), *TGAS100* (g), *bHLH89/91* (h), *TA29* (i), *Cysteine protease* (j), *Aspartic proteinase* (k), and *Arabinogalactan protein* (l) genes. The results show the averages and standard errors of three independent biological experiments and three technical replicates. Asterisks denote significant differences (Student's t-test, $P < 0.05$).

Figure 7. Expression of the tomato *SlMED18* rescues the phenotype defects displayed by Arabidopsis *med18-1* plants. Compared to wild-type plants (Columbia), no visible differences were found in the Arabidopsis *med18-1* plants overexpressing tomato *SlMED18* (35S::*SlMED18 med18-1*) with respect to flowering time (a), identity and number of floral organs (b), fruit size (c,f), and number of leaves before flowering (d,e).
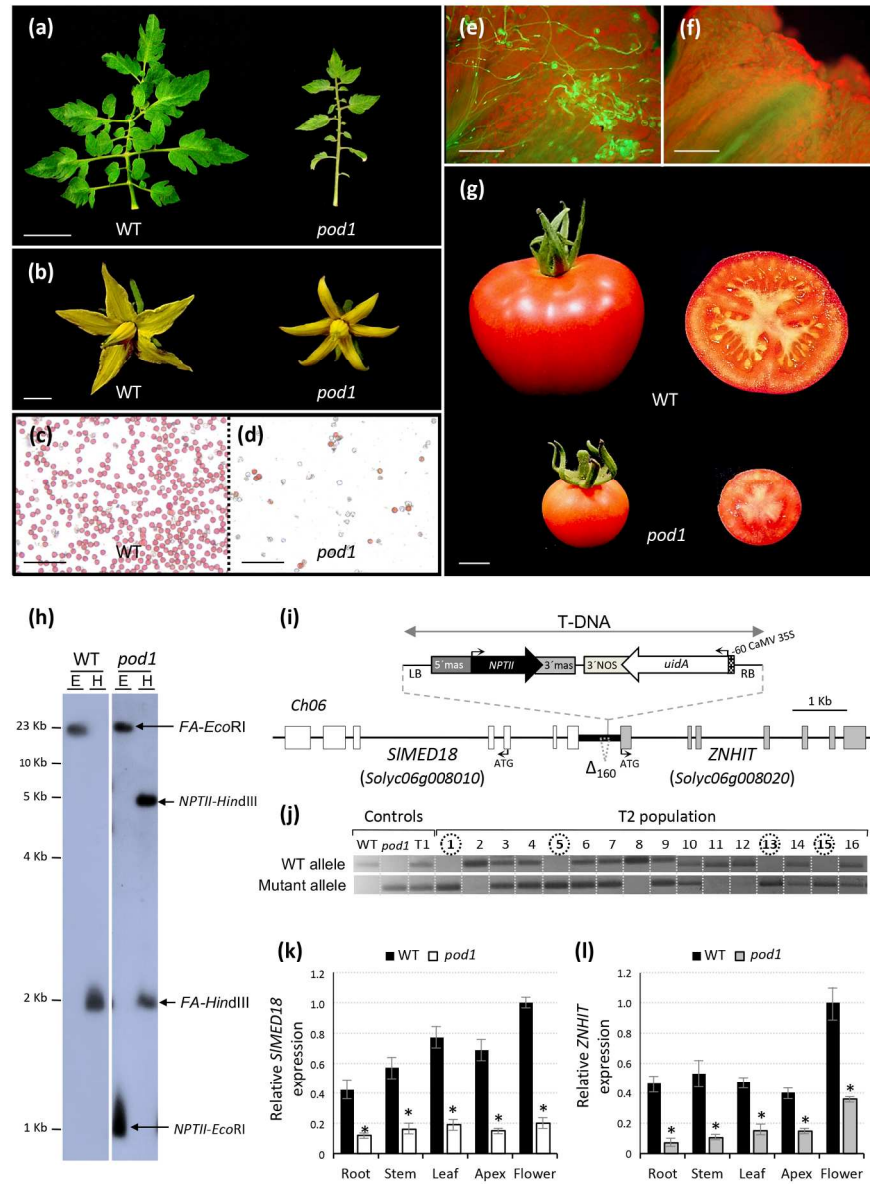
Figure 1. Phenotypic and molecular characterization of pod1 insertional mutant
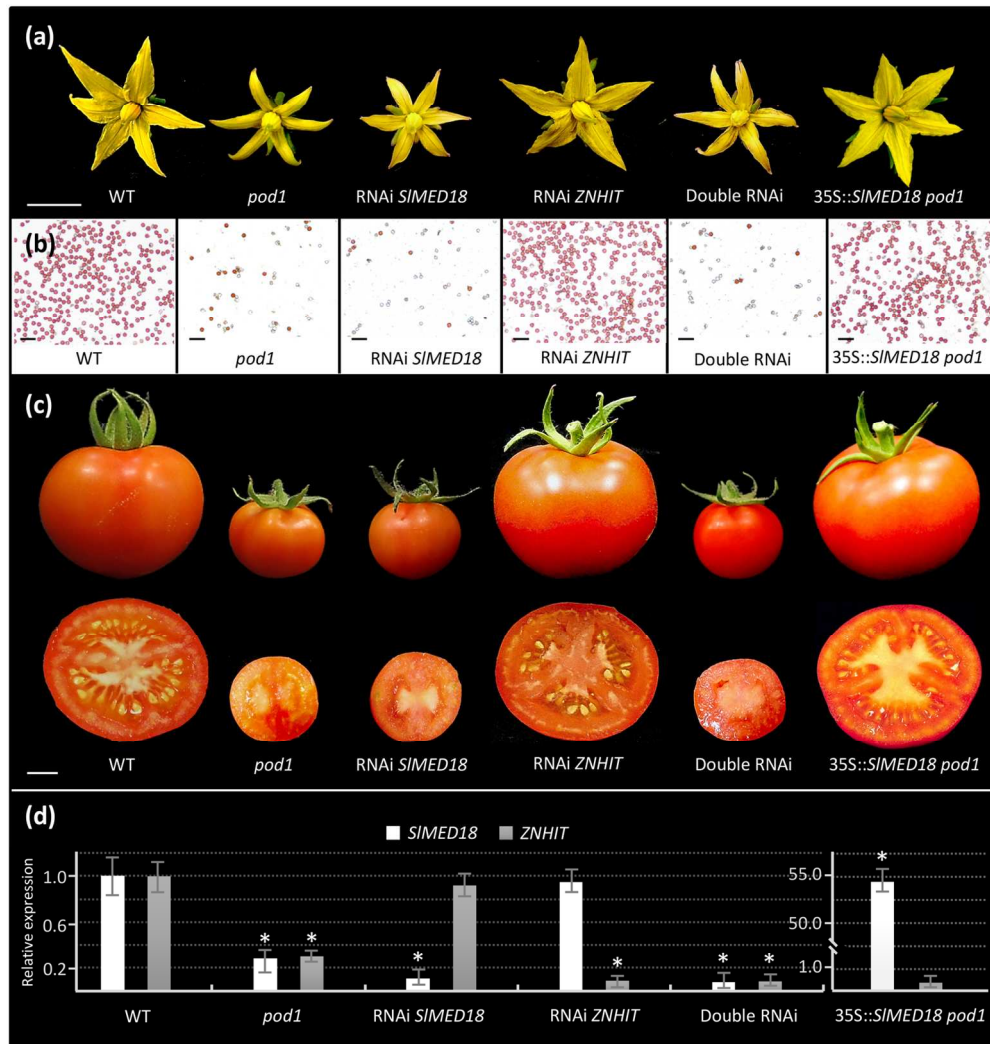
161x219mm (300 x 300 DPI)

Figure 2. *SlMED18* silencing plants phenocopy the *pod1* mutant phenotype
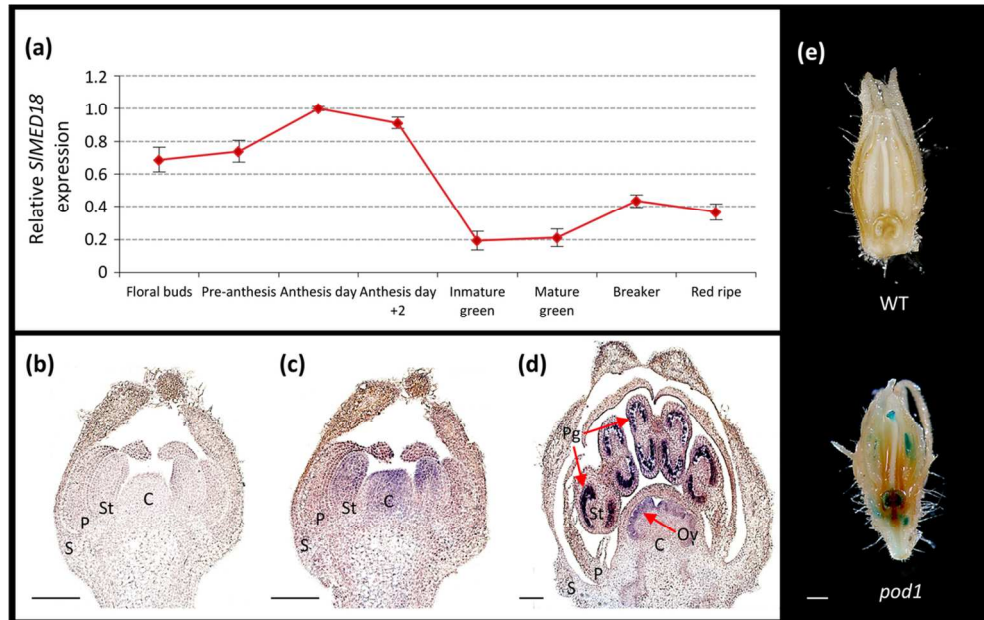
136x144mm (300 x 300 DPI)

Figure 3. Expression of *SlMED18* in reproductive floral organs
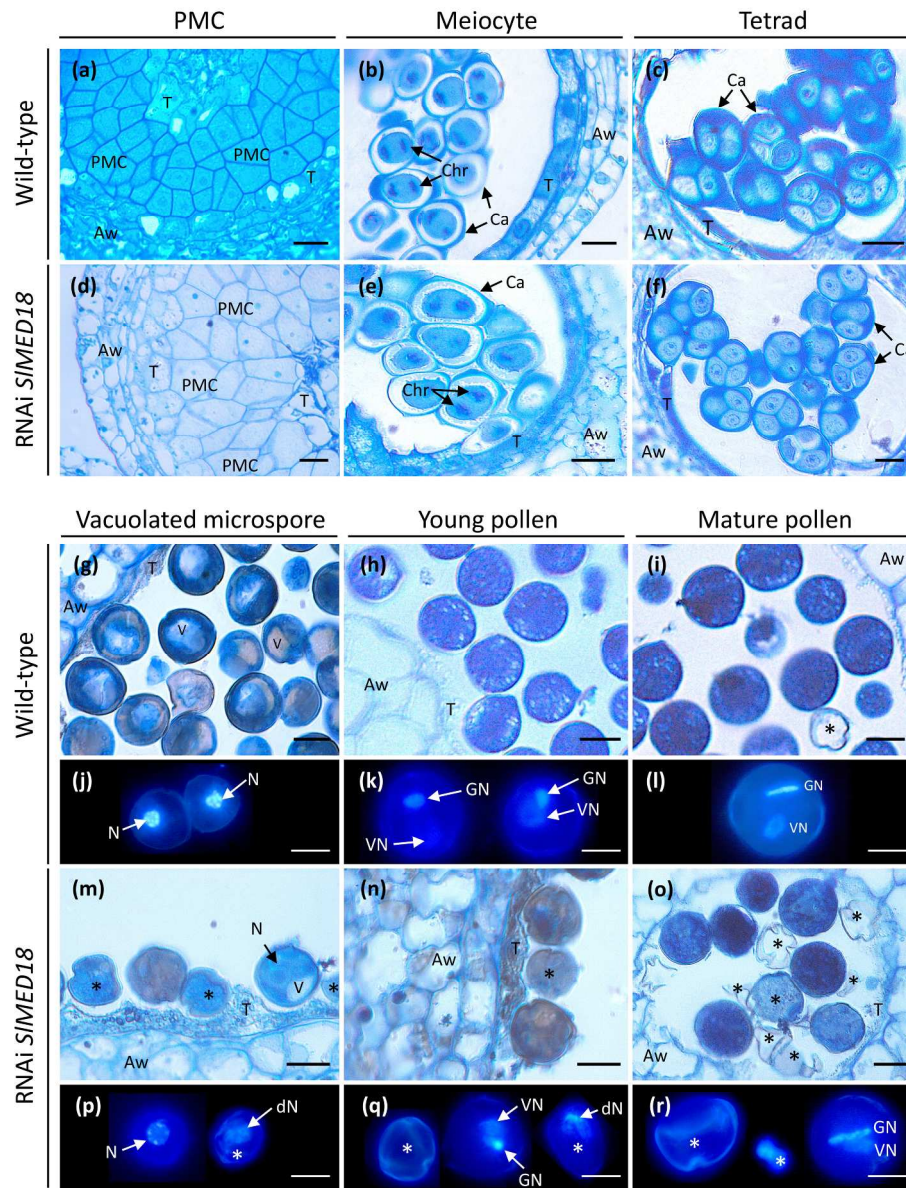
104x66mm (300 x 300 DPI)

Figure 4. Microscopy analysis of microsporogenesis and microgametogenesis in wild-type and RNAi *SlMED18* plants
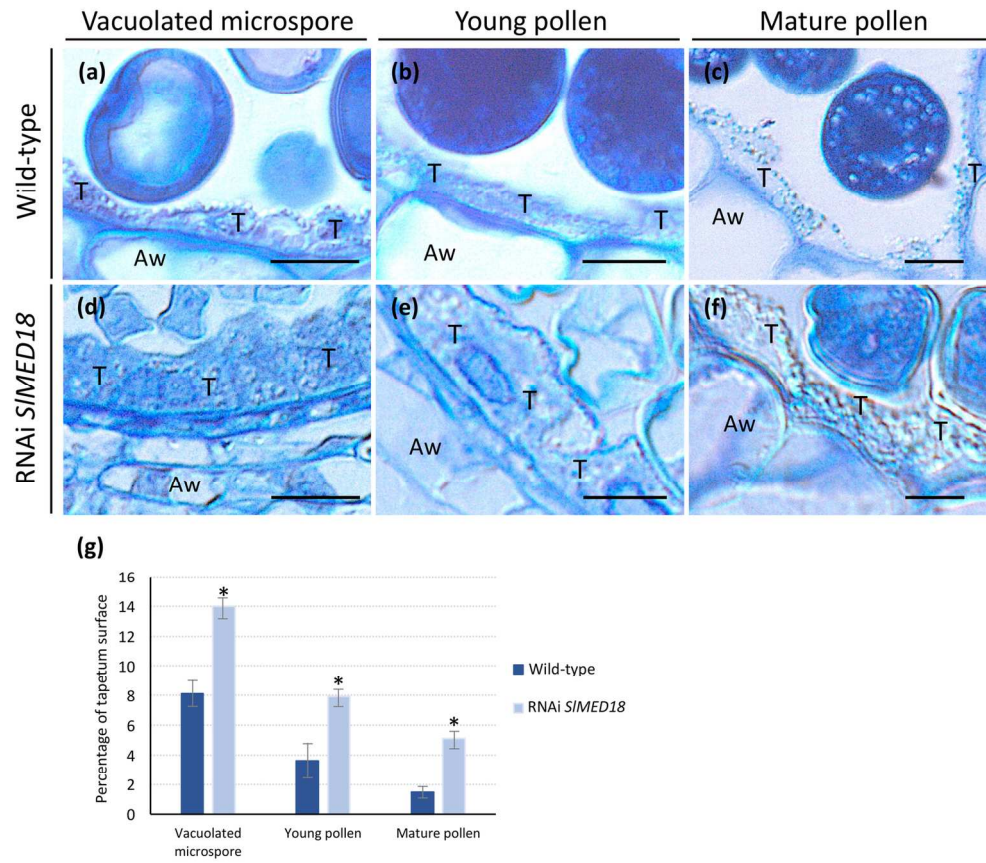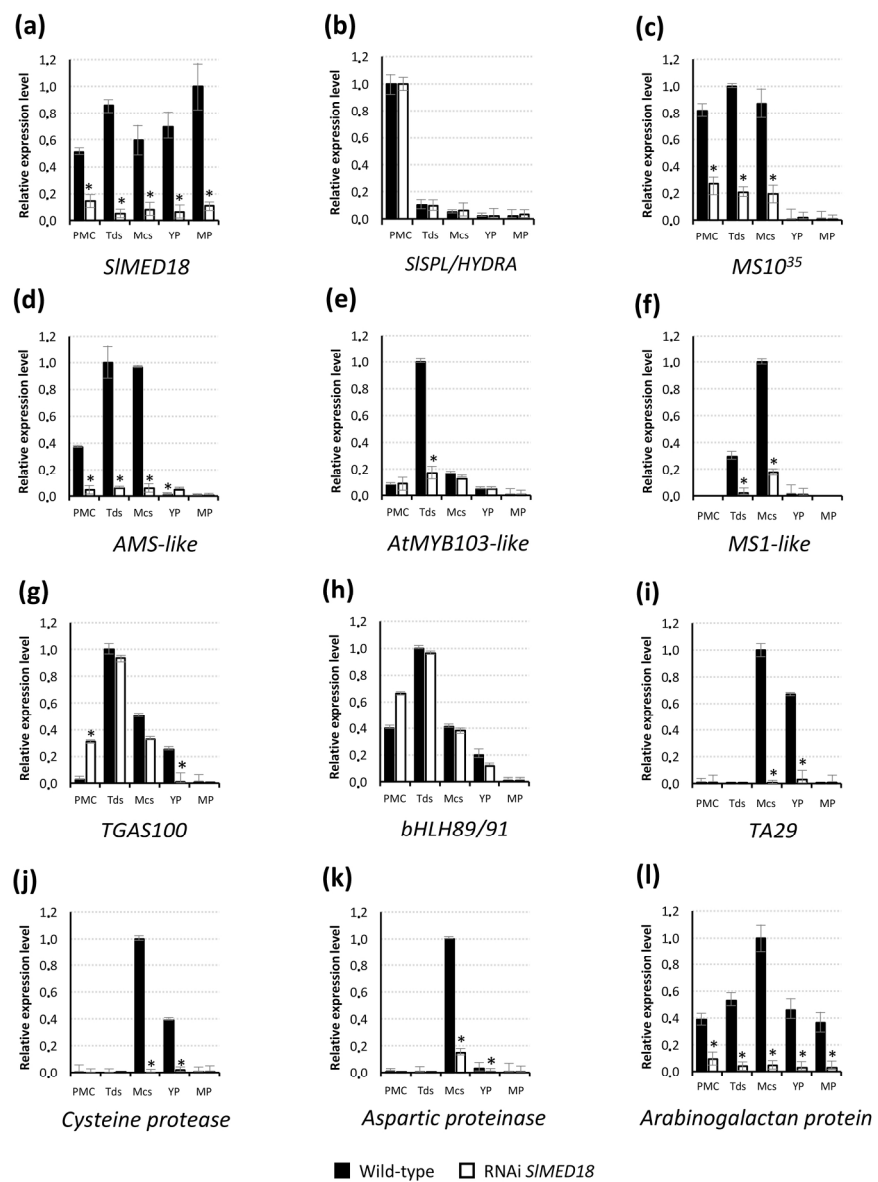
221x289mm (300 x 300 DPI)

| | Vacuolated microspore | Young pollen | Mature pollen |

Wild-type

(a) T T T Aw

(b) T T Aw

(c) T T Aw

RNAi *SlMED18*

(d) T T T Aw

(e) T T Aw T

(f) T T Aw T

(g)

Figure 5. Tapetum development is altered during microgametogenesis of RNAi *SlMED18* plants

147x129mm (300 x 300 DPI)

Figure 6. Expression of tapetum marker genes in wild-type and RNAi *SlMED18* plants
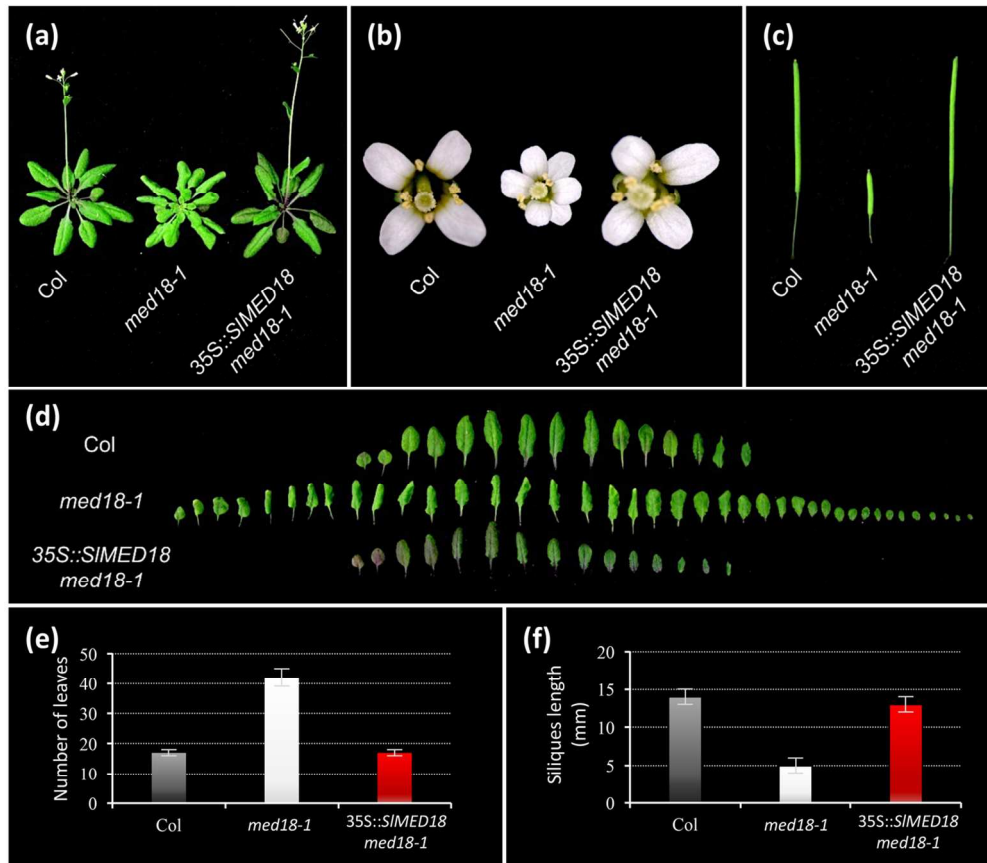
179x241mm (300 x 300 DPI)

Figure 7. Expression of the tomato *SlMED18* rescues the phenotype defects displayed by Arabidopsis *med18-1* plants

120x104mm (300 x 300 DPI)

Significance statement

Pollination is a key development process in the life cycle of flowering plants. Genetic and molecular characterization of a tomato mutant have led to the identification of *POD1* gene encoding the Mediator complex subunit MED18 whose function is required for tapetum tissue degeneration, a crucial step for pollen development. Furthermore, we show that MED18 fulfils an essential role in tomato, ensuring proper gene regulation during pollen ontogeny.
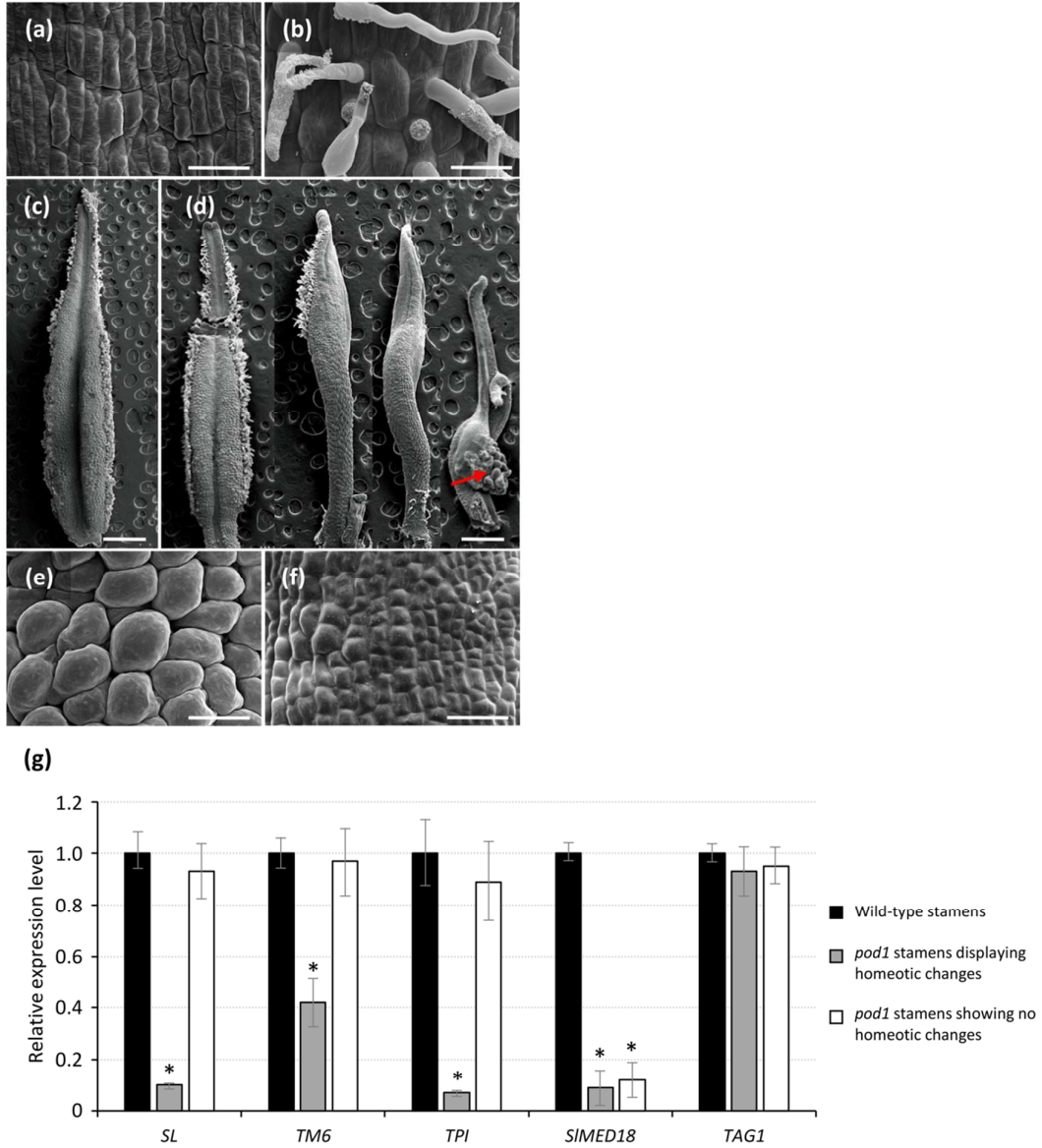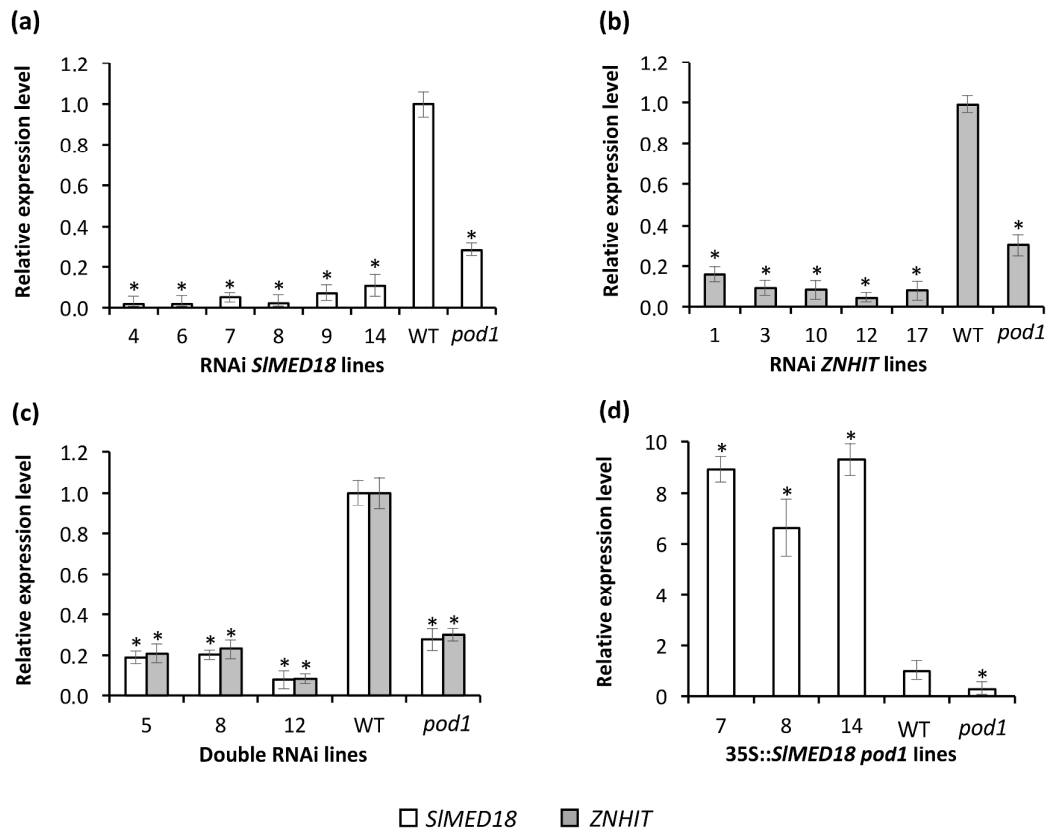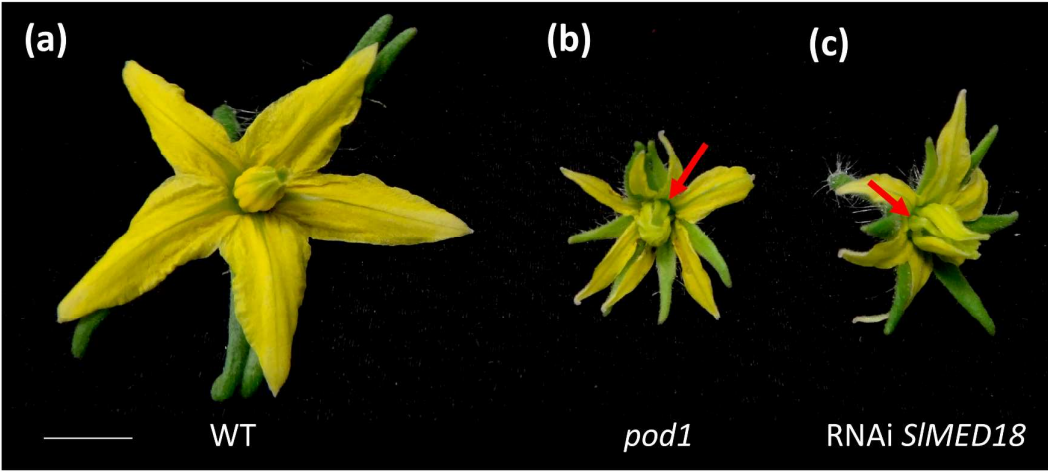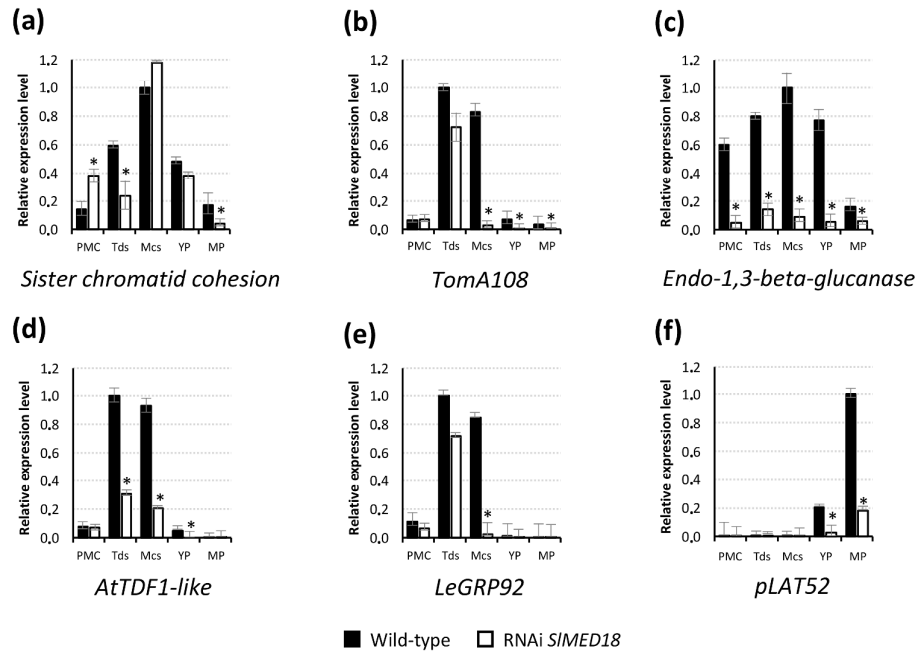
Figure S1

Figure S2

Figure S3

(a) Sister chromatid cohesion

(b) TomA108

(c) Endo-1,3-beta-glucanase

(d) AtTDF1-like

(e) LeGRP92

(f) pLAT52

■ Wild-type □ RNAi SlMED18

Figure S4

Figure S5

(a)

(b)
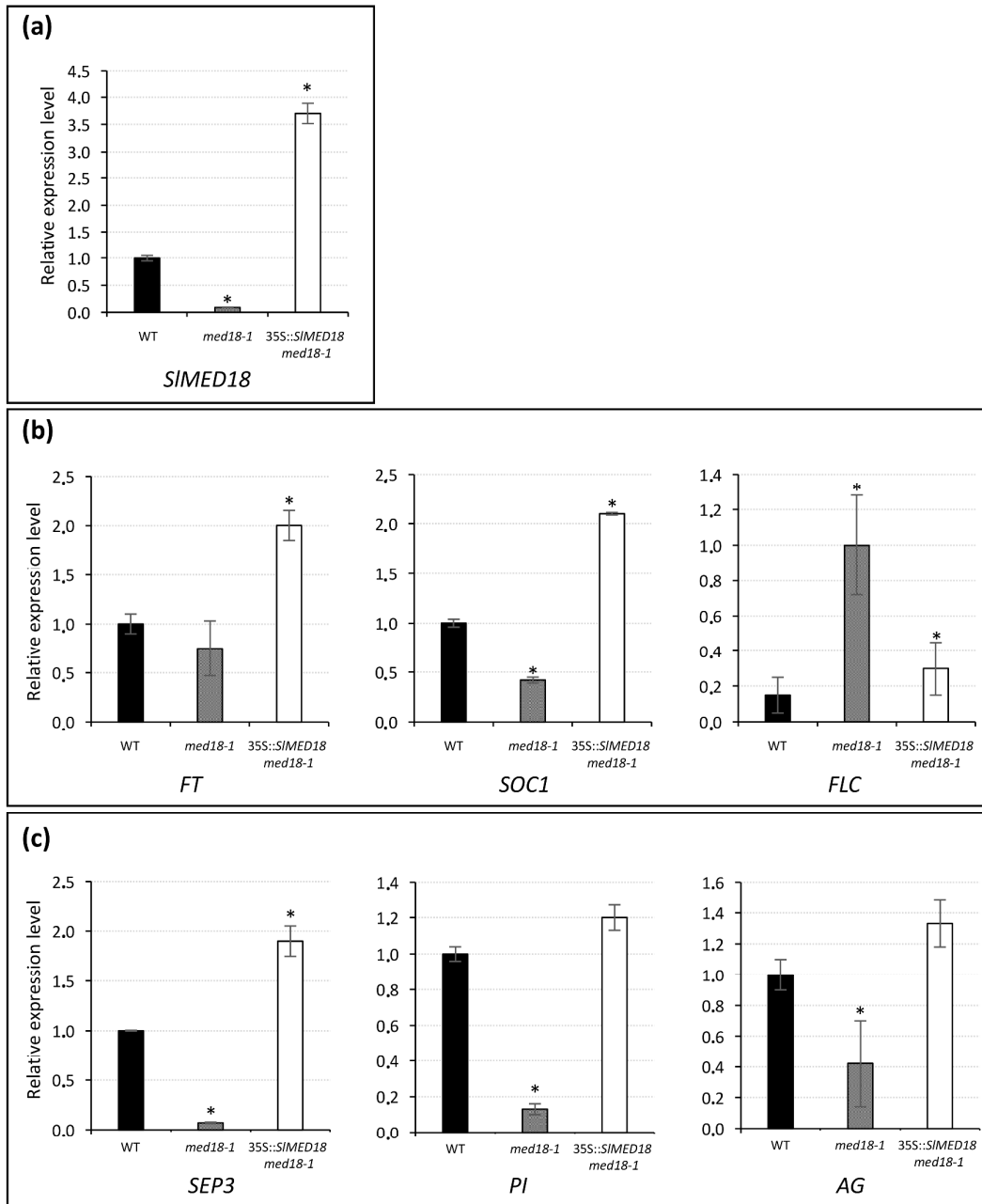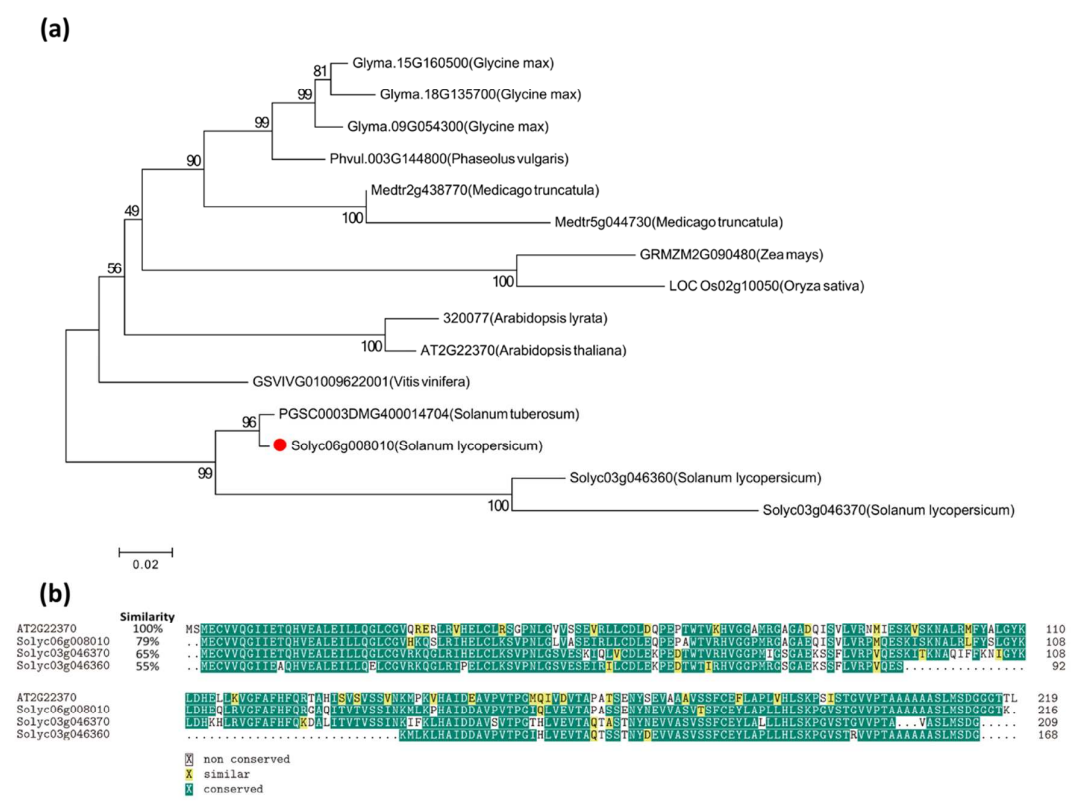
Figure S6

Table S1

Category	Wild-type	*pod1*	RNAi *ZNHIT*	RNAi *SlMED18*	Double RNAi	35S::*SlMED18 pod1*
Fresh weight of leaf (g)	54.31 ± 12.92^a	19.68 ± 5.97^b	50.98 ± 11.03^a	21.33 ± 7.01^b	20.16 ± 6.45^b	55.12 ± 9.14^a

Values are expressed as the mean ± standard deviation. Values followed by the same letter ([a], [b], or [c]) are not statistically different (Least significant difference test, *P*<0.01).

Length of leaf (mm)	491.83 ± 39.54[a]	347.5 ± 46.58[b]	477.91 ± 42.22[a]	360.1 ± 37.11[b]	355.8 ± 54.22[b]	489.25 ± 41.69[a]
Length of petiole (mm)	58.40 ± 1.08[a]	37.77 ± 3.20[b]	56.16 ± 2.23[a]	36.16 ± 3.84[b]	38.01 ± 2.99[b]	54.10 ± 1.56[a]
Length of secondary petiole (mm)	27.01 ± 2.40[a]	12.50 ± 1.20[b]	25.94 ± 3.56[a]	11.85 ± 3.72[b]	14.31 ± 3.02[b]	24.98 ± 3.11[a]
Length of sepal (mm)	9.81 ± 0.55[a]	9.46 ± 2.04[a]	9.47 ± 1.26[a]	9.77 ± 1.85[a]	9.97 ± 2.05[a]	9.63 ± 1.67[a]
Length of petal (mm)	14.80 ± 1.30[a]	13.16 ± 1.57[b]	14.56 ± 0.73[a]	12.85 ± 1.60[b]	13.04 ± 1.16[b]	14.80 ± 1.30[a]
Length of stamen (mm)	8.46 ± 1.60[a]	6.64 ± 1.30[b]	8.50 ± 0.49[a]	7.71 ± 1.03[c]	7.67 ± 0.83[c]	8.18 ± 1.00[a]
Length of pistil (mm)	7.18 ± 0.55[a]	5.26 ± 0.50[b]	7.68 ± 0.83[a]	6.07 ± 1.09[c]	6.19 ± 1.31[c]	7.34 ± 0.91[a]
Diameter of peduncle (mm)	0.71 ± 0.06[a]	1.20 ± 0.20[b]	0.75 ± 0.23[a]	1.00 ± 0.16[c]	0.96 ± 0.20[c]	0.68 ± 0.15[a]
Diameter of carpel (mm)	1.63 ± 0.24[a]	1.63 ± 0.26[a]	1.58 ± 0.32[a]	1.60 ± 0.22[a]	1.66 ± 0.27[a]	1.59 ± 0.28[a]
Axial diameter of fruit (mm)	47.97 ± 2.82[a]	28.75 ± 2.06[b]	52.50 ± 1.32[a]	27.12 ± 1.30[b]	28.68 ± 2.10[b]	50.07 ± 3.05[a]
Equatorial diameter of fruit (mm)	59.44 ± 4.28[a]	31.40 ± 5.83[b]	62.33 ± 2.88[a]	30.88 ± 1.52[b]	32.03 ± 1.79[b]	61.28 ± 3.87[a]
Fresh weight of fruit (g)	130.75 ± 19.09[a]	18.90 ± 5.90[b]	134.59 ± 17.92[a]	19.61 ± 1.95[b]	20.07 ± 1.89[b]	133.05 ± 18.51[a]
Relative amount of pollen (%)	98.30 ± 5.20[a]	17.60 ± 9.10[b]	98.20 ± 7.30[a]	14.30 ± 6.20[b]	16.30 ± 6.40[b]	93.90 ± 5.80[a]
Pollen viability (%)	97.60 ± 3.60[a]	28.70 ± 12.40[b]	96.20 ± 4.10[a]	18.70 ± 8.80[b]	15.70 ± 9.90[b]	96.50 ± 3.60[a]

Table S2

(a) Primers used for anchor-PCR	
Primer name	Primer sequence 5`-3`
Ad1	CTAATACGACTCACTATAGGC
Ad2	CTATAGGGCTCGAGCGGC
Ad3	AGCGGCGGGGAGGT
ARB-1	ACAGTTTTCGCGATCCAGAC
ARB-2	GGTCTTGCGAAGGATAGTGG
ARB-3	CTGGCGTAATAGCGAAGAGG
ALB-1	TTGGCGTGTCAGCGTATCTA
ALB-2	ATCGGTCTCAATGCAAAAGG
ALB-3	ATAATAACGCTGCGGACATCTAC

(b) Primers used for PCR genotyping analysis	
Primer name	Primer sequence 5`-3`
619a_genot_F	TCAACAGTAAAAACGAGCCAAA
619a_genot_R	GGATGAAGCAATTGGGACAC
RB_pD991_F	TACAACGTCGTGATGGGAAA

(c) Primers used for generation of transgenic lines	
Primer name	Primer sequence 5`-3`
RNAiMED18_F	tctagactcgagTTCTTTGGCTCGTTGTTATCG
RNAiMED18_R	atcgatggtaccTTGAACAGTTGAAGCAATCTCA
RNAiZn_F	tctagactcgagTGGAGAAGTTCAACAGGATACG
RNAiZn_R	atcgatggtaccAATGGAAGCAGAAGCAGAGG
RNAi-doble_F	gctagtcgcgaggcTTCTTTGGCTCGTTGTTATCG
RNAi-doble_R	gcctcgcgactagcAATGGAAGCAGAAGCAGAGG
35S-Med_F	ggtaccAAAAATCTCTCTTTGGCTCGTTT
35S-Med_R	gagctcCTGCTGTGCTTTGTTTTTCG

* In lowercase is shown the endonuclease site introduced in the primer sequence

Table S3

Locus	Forward primer sequence 5'- 3'	Reverse primer sequence 5'- 3'	SGN id
SlAMS-like	TGCAGAGATGTTATGTTTCAGCATC	TCGTCTCTGTCTCTTTCTCCTTCTG	*Solyc08g062780*
SlMS1-like	TTGTGTCAATGGATCATTGGAAAC	AACCTCTTGCCTAGACACCCATC	*Solyc04g008420*
Slendo13bGl	GATCCAATGTGGGGAAGAAA	CCACAAATCAAAGCACCTCA	*Solyc03g046200*
SlpLAT52	AAGGTGTGACTGATAAAGATGGC	AACCCAACTCATCAAGAGCTTC	*Solyc10g007270*
SlbHLH89/91	TCCATGGATGGTAGTGATGC	TCGACAATCCGAACATCAAC	*Solyc01g081100*
SlCysProt	ATTGGTGTCGATTGGAGGAAG	CAAATGCACTTTCCATAAACCC	*Solyc07g053460*
SlAspProt	GTGATATTAATTGGCTTCAATGTGAACC	ATACTCGCCGGAACCTGTAACATC	*Solyc06g069220*
SlTA29	AAGATTTTAACCATGAACTTCTTC	ACATTCTTCAGTGTCACATACATC	*Solyc02g078370*
SlTomA108	ATGCAATTAGGAGCCTTGATTC	CAGTTCCAGTTCCTGTTCCG	*Solyc01g009590*
SlTGAS100	TATATAGACATGGCAATGAAATGGC	AGTCAAGACAACGATCAAGAATGC	*Solyc06g064480*
SlSisterCC	CATTGGCTTTCAGAGCTTCC	GCAGCAGAAAGCGAAATTCT	*Solyc03g116930*
LeGRP92	ATGCAATTAGGAGCCTTGATTC	CAGTTCCAGTTCCTGTTCCG	*Solyc02g032910*
SlMS10-35	AGATCTCTCTGATTCGATTAGCTTCAG	TCTTGAAATGGAAGCAACTCAGG	*Solyc02g079810*
SlTDF1-like	GGTAATTGGGCAACCATGTC	TTGAGGCGTAAAGCTGTCCT	*Solyc03g113530*
SlMYB103-like	TGCTGAGGAAGATGCAAAAA	GGTCCATCTCAGCCTACAGC	*Solyc03g059200*
SlArabinogalProt	CCTTTTCATTCTGGGGTGAC	CGTCACTAACAACCTTTGAACG	*Solyc11g072780*
619a_ZFinger	AGCTGTGTAAGGCGTGCTCT	ACAGCTATATCGATCACACTTCGTTT	*Solyc06g008020*
SlMED18	TCTCTGATGTCTGATGGTGGA	GAAGGAGAATGGCGAAATAC	*Solyc06g008010*
AtMED18	CGAACCCACATGGACGGTTAAA	AGATGAAACAGCAGCAGCGACT	*AT2G22370*
FT	CATCGTGTCGTGTTTATATTGTTTCG	CCTCCGCAGCCACTCTCC	*AT1G65480*
SOC1	ACTCTTGGGAGAAGGCATAGGA	TGGGCTACTCTCTTCATCACCT	*AT2G45660*
FLC	TCACCTTCTCCAAACGTCGCAA	TGAGTTCGGTCTTCTTGGCTCT	*AT5G10140*
SEP3	ACGCCTTACAGAGAACCCAAAGGA	TTTGTCTCAGTCAGCATGCGTTCC	*AT1G24260*
PI	ACCAATGCTCCTCTTCTTGTTCTTC	ACTCTGTTGTTTGCGTTCTCTATCC	*AT5G20240*
AG	CGAGTATAAGTCTAATGCCAGGAG	GAGTAATGGTGATTGTTAGGTTGC	*AT4G18960*
TM6	GGAAAAATTGAGATCAAGAAG	TCAGGAGAGACGTAGATCAC	*Solyc02g085480*
TPI	TGGGGAGAGGTAAAATAGAG	GTAGATTTGGCTGCATTGGC	*Solyc06g059970*
SL (AP3)	ATGGCTCGTGGTAAGATCCAG	TCAACCTAGAGCAAAAGTAG	*Solyc04g081000*
UBC21	CTTGGACGCTTCAGTCTGTG	TGAACCCTCTCACATCACCA	*AT5G25760*
Ubiquitine3	CACACTTCACTTGGTCTTGCGT	TAGTCTTTCCGGTGAGAGTCTTCA	*Solyc01g056940*